The Astronomical Journal, 126:2060–2080, 2003 October

UPGRADES TO THE FLAGSTAFF ASTROMETRIC SCANNING TRANSIT TELESCOPE: A FULLY AUTOMATED TELESCOPE FOR ASTROMETRY

Ronald C. Stone, David G. Monet, Alice K. B. Monet, Frederick H. Harris, Harold D. Ables, Conard C. Dahn, Blaise Canzian, Harry H. Guetter, Hugh C. Harris, Arne A. Henden,[1] Steven E. Levine, Christian B. Luginbuhl, Jeffrey A. Munn, Jeffrey R. Pier, Frederick J. Vrba, and Richard L. Walker
US Naval Observatory, Flagstaff Station, P.O. Box 1149, Flagstaff, Arizona 86002; rcs@nofs.navy.mil
Received 2003 April 10; accepted 2003 June 19

ABSTRACT

The Flagstaff Astrometric Scanning Transit Telescope (FASTT) is a fully automated telescope that takes about 41,000 CCD frames of data a year for various research projects. All aspects of the telescope's operation have been automated (e.g., target selection, observing, reduction of data, and collation of results), and manpower needs are now under one person per year, mostly involved with routine maintenance and the dissemination of data. This paper describes the FASTT instrumental system, methods used with its automated operation, and the various FASTT research projects. Among the projects, astrometry is provided in support of various spacecraft missions, to predict occultation events, calculate dynamical masses for selective asteroids, and improve the ephemerides for thousands of asteroids, the planets Jupiter to Pluto, and 17 satellites of Jupiter through Neptune. Although most of the FASTT observing program involves the solar system, FASTT stellar astrometry was used to set up a number of astrometric calibration regions along the celestial equator, verify the *Hipparcos* link to the International Celestial Reference Frame, determine accurate positions for a large sample of radio stars, and investigate systematic errors in the FK5 star catalog. Furthermore, the FASTT produces accurate magnitudes that are being used to investigate the shapes of thousands of asteroids. By the end of year 2003, the FASTT will have produced over 190,000 positions of solar system objects in a program to provide a very large and homogeneous database for each object that will extend over many years and include positions accurate to ± 47 to ± 300 mas, depending on the magnitude of each observed object ($3.5 < V < 17.5$). Moreover, extensive efforts have been undertaken to improve the systematic accuracy of FASTT equatorial positions by applying corrections in the reductions for differential color refraction, distortions in the focal plane, and correcting for a positional error that is dependent on magnitude. The systematic accuracy of FASTT observations is now about ± 20 mas in both right ascension and declination. FASTT data have contributed very significantly to recent successful spacecraft missions and to a dramatic improvement in the predictions made for occultation events.

Key words: astrometry — instrumentation: detectors — methods: data analysis — methods: observational — techniques: image processing — techniques: photometric

1. INTRODUCTION

The Flagstaff Astrometric Scanning Transit Telescope (FASTT) is a traditional meridian telescope that has been modified to observe in drift-scan mode and is now a fully automated instrument that provides many thousands of observations each year of exceptional quality. The telescope was upgraded in 1989 to observe with a CRAF/Cassini 1024^2 charge-coupled device (CCD) and used then as a test bed instrument to learn about drift scanning and, in particular, its application to astrometry. The US Naval Observatory (USNO) planned to build a large digital astrograph, and knowledge obtained from the FASTT was needed to design such an instrument. At that time, CCDs were relatively small and CCD mosaics difficult and costly to built. In order to survey large regions of the sky, scan observing was considered, and numerous tests were undertaken with the FASTT exploring this method of gathering CCD data (Stone et al. 1996). Although tests with the FASTT showed that scanning up to the celestial pole was possible, the idea of scan observing at the observatory was abandoned because of the subsequent development of large-format CCDs that offered a faster and more accurate means to survey the sky.

A second part of the early FASTT program was to develop techniques for fully automated observing. Normally, automated observing is associated with the taking of data automatically, but the FASTT concept would include all other aspects of telescope operation as well (e.g., selection of targets, reductions to final positions and magnitudes, and the collations of data). In time, all these goals were achieved. Prior to the release of the *Hipparcos* Catalogue (ESA 1997a), star positions were obtained using either traditional meridian telescopes or astrographs and catalogs such as the FK5 (Fricke, Schwan, & Lederle 1988). Since the FASTT could observe considerably fainter stars than those telescopes, a wide-angle program was set up that used radio reference sources in the reductions, comprising the most accurate positions available at the time. The resulting FASTT positions were accurate to ± 160 mas, in general, a value not much larger than the limit imposed by atmospheric refraction (Stone et al. 1996). FASTT positions were among the best being produced at the time, and as a result, the FASTT was tasked for a number of observing projects, which included the establishment of astrometric calibration

[1] Universities Space Research Association.

Report Documentation Page

Form Approved
OMB No. 0704-0188

1. REPORT DATE	2. REPORT TYPE	3. DATES COVERED
OCT 2003		**00-00-2003 to 00-00-2003**

4. TITLE AND SUBTITLE	5a. CONTRACT NUMBER
Upgrades To The Flaggstaff Astrometric Scanning Transit Telescope: A Fully Automated Telescope For Astrometry	5b. GRANT NUMBER
	5c. PROGRAM ELEMENT NUMBER
6. AUTHOR(S)	5d. PROJECT NUMBER
	5e. TASK NUMBER
	5f. WORK UNIT NUMBER
7. PERFORMING ORGANIZATION NAME(S) AND ADDRESS(ES) **US Naval Observatory,Flagstaff Station,P.O. Box 1149,Flagstaff,AZ,86002**	8. PERFORMING ORGANIZATION REPORT NUMBER
9. SPONSORING/MONITORING AGENCY NAME(S) AND ADDRESS(ES)	10. SPONSOR/MONITOR'S ACRONYM(S)
	11. SPONSOR/MONITOR'S REPORT NUMBER(S)

12. DISTRIBUTION/AVAILABILITY STATEMENT
Approved for public release; distribution unlimited

13. SUPPLEMENTARY NOTES
The Astronomical Journal, Volume 126, Issue 4, pp. 2060-2080,2003 October

14. ABSTRACT

The Flagstaff Astrometric Scanning Transit Telescope (FASTT) is a fully automated telescope that takes about 41,000 CCD frames of data a year for various research projects. All aspects of the telescope's operation have been automated (e.g., target selection, observing, reduction of data, and collation of results), and manpower needs are now under one person per year, mostly involved with routine maintenance and the dissemination of data. This paper describes the FASTT instrumental system, methods used with its automated operation, and the various FASTT research projects. Among the projects, astrometry is provided in support of various spacecraft missions, to predict occultation events, calculate dynamical masses for selective asteroids, and improve the ephemerides for thousands of asteroids, the planets Jupiter to Pluto, and 17 satellites of Jupiter through Neptune. Although most of the FASTT observing program involves the solar system, FASTT stellar astrometry was used to set up a number of astrometric calibration regions along the celestial equator, verify the Hipparcos link to the International Celestial Reference Frame, determine accurate positions for a large sample of radio stars, and investigate systematic errors in the FK5 star catalog. Furthermore, the FASTT produces accurate magnitudes that are being used to investigate the shapes of thousands of asteroids. By the end of year 2003, the FASTT will have produced over 190,000 positions of solar system objects in a program to provide a very large and homogeneous database for each object that will extend over many years and include positions accurate to +/-47 to +/-300 mas, depending on the magnitude of each observed object (3.5<V<17.5). Moreover, extensive efforts have been undertaken to improve the systematic accuracy of FASTT equatorial positions by applying corrections in the reductions for differential color refraction, distortions in the focal plane, and correcting for a positional error that is dependent on magnitude. The systematic accuracy of FASTT observations is now about +/-20 mas in both right ascension and declination. FASTT data have contributed very significantly to recent successful spacecraft missions and to a dramatic improvement in the predictions made for occultation events.

15. SUBJECT TERMS

16. SECURITY CLASSIFICATION OF:			17. LIMITATION OF ABSTRACT	18. NUMBER OF PAGES	19a. NAME OF RESPONSIBLE PERSON
a. REPORT	b. ABSTRACT	c. THIS PAGE			
unclassified	**unclassified**	**unclassified**	**Same as Report (SAR)**	**22**	

fields for the Sloan Digital Sky Survey (SDSS) discussed in Stone, Pier, & Monet (1999b), support for NASA spacecraft missions (Monet et al. 1994; Stone 1997a), investigation of the link to the International Celestial Reference System (ICRS) reference frame (Stone 1994, 1997c, 1998b), and provision of accurate positions for solar system objects (Stone 1996b, 1997a, 2000a, 2000b, 2001), among other assignments. A very comprehensive paper describing the FASTT was published in Stone et al. (1996).

Despite its small size, the FASTT has continued to survive, since it produces copious amounts of highly accurate astrometry for numerous projects with scientific merit, and operational costs are minimal, because all aspects of its operation have been automated. Furthermore, the FASTT has a rapid turnaround time for providing data, where positions are usually available the morning after a request for data is received. Much can be learned from the improvements made to the FASTT starting in 1997, wherein all the astrometry is now referred to the Tycho-2 Catalogue (Høg et al. 2000) using differential reductions. On average, the FASTT takes about 41,000 CCD frames of data a year with an efficiency of about 97%, that is, the likelihood that the FASTT will successfully get data on a clear night.

This paper describes improvements made to the FASTT since the Stone et al. (1996) paper and gives more details about the automated operation of the instrument. Section 2 describes the current state of the telescope instrumentation, including the large-format Ford-Loral CCD now in use; the two types of drift-scan observing used with the FASTT are discussed in § 3; § 4 describes FASTT automated systems for scheduling the observations, taking the observations, reducing the data, applying quality checks, and collating the final positions and magnitudes; a discussion of FASTT errors is presented in § 5; § 6 discusses various FASTT observing programs; and finally, concluding remarks are given in the final section of the paper.

2. INSTRUMENTATION AND OBSERVING SITE

The FASTT is a 20 cm achromatic telescope with a focal scale of 99 arcsec mm^{-1} and is equipped with a front-illuminated Ford-Loral 2048^2 CCD with 15 μm pixels, giving the instrument a $50\farcm7 \times 50\farcm7$ field of view. Further details about the instrument are presented in Table 1. The telescope was constructed originally for wide-angle positional astrometry, and, to achieve a high degree of stability, it was designed as to observe only along the celestial meridian. Moreover, because the CCD is fixed in the camera head, the FASTT can observe only in drift-scan mode. Cosmetically, the CCD is very good (fewer than 0.08% of the pixels are bad), but it does have a charge transfer efficiency (CTE) problem, wherein charge images have a tail in the direction of the serial readout. This problem can be greatly ameliorated by raising the operating temperature of the device, but as a downside, the readout noise will be increased. By experimentation, a CCD operating temperature of -49° C was chosen as the best compromise between the two trade-offs and is achieved with thermoelectric cooling. The resulting images have no apparent tails, and the noise floor has been raised only slightly. Nonetheless, there is a residual effect that produces a small systematic error that affects declinations determined with the FASTT, which will be discussed in § 4.4.3.

TABLE 1
CHARACTERISTICS OF THE FASTT

Characteristic	Value
Aperture	20 cm
Scale	99 arcsec mm^{-1}
Focal ratio	f/10
CCD field of view	$50\farcm7 \times 50\farcm7$
CCD	Ford-Loral 2048 × 2048 with antiblooming
CCD cooling	Thermoelectric to -49°C
Pixel size	15 μm ($1\farcs486$)
Gain	3.65 e^- DN^{-1}
Readout noise	11 e^-
Typical stellar FWHM	2.8 pixels
Passband (F606W)	4700–7300 Å
Magnitude compensation	3.9 mag neutral density filter
Exposure times used	10–202 s
Magnitude range	$3.5 < V < 17.7$
Reference frame	ICRS (Tycho-2 reference catalog)
Declinations observed	$\delta > -45^\circ$

As discussed in § 6, the FASTT is involved in many observing projects, and one of these projects is to observe satellites of the outer planets Jupiter, Saturn, Uranus, and Neptune. A serious problem occurs when a satellite falls within the bloomed streak of the saturated planet, causing the satellite's image to be lost. In order to remedy this problem, the electronics supporting the Ford-Loral CCD have been modified to include clocked antiblooming logic. The antiblooming works extremely well by keeping saturated planetary images within their limb boundaries, and as a result satellites can be observed now quite close to their parent planets in all possible orientations.

The incident light is filtered with a *Hubble Space Telescope* F606W filter that gives the FASTT a very broad passband (4700–7300 Å) and a limiting magnitude $V \sim 17.7$ that goes quite deep, considering that the FASTT is only a 20 cm telescope. Figure 1 shows the response of the filter. Under normal operation, objects brighter than $V \sim 7.5$ saturate; however, a 3.9 mag neutral density filter can be mechanically swung into the optical path so that objects as bright as $V \sim 3.5$ can be observed with the FASTT. The chosen broad passband causes some of the light to be defocused because of chromatic aberrations. Based on years of experience, this does not seem to affect the astrometry, and, in fact, it offers an advantage, wherein the full width at half-maximum (FWHM) is increased to about 2.8 pixels because of the defocusing. Without the defocusing FASTT images would be badly undersampled (FWHM < 1.0 pixel) on nights with $\phi < 1\farcs5$ seeing, which are quite common at the observing site.

Other data are collected automatically in the course of FASTT operation. Throughout the night, readings of ambient temperature, barometric pressure, and dew point are taken every 30 s and recorded to a data file. These data are needed when applying corrections for refraction in the astrometric reductions (see § 4.3 for details). Moreover, there is a flat screen located within the telescope enclosure that is used to take flats. After the telescope is pointed toward the screen, illuminating lamps are turned on and a series of flat CCD frames are taken each observing night.

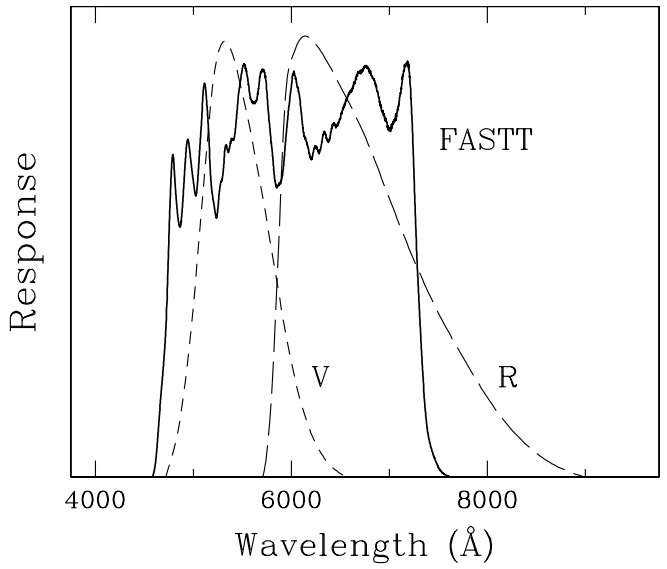

FIG. 1.—Diagram showing the FASTT passband compared with the standard Johnson V and Cousins R passbands. The FASTT passband was chosen purposely to be wide (FWHM = 2600 Å) so that objects as faint as $V \sim 17.7$ could be reached.

All aspects of the telescope's operation have been automated, and manpower needs are now less than one person per year. In fact, the telescope can be, and has been, operated for weeks on end without supervision. Manpower needs comprise routine maintenance, the periodic editing of observations, and the timely dissemination of results to the astronomical community. Concerning its operation, the telescope is driven to each setting with a stepper motor connected to its axis of rotation through a gear train, while the position of the telescope is monitored with a high-resolution BEI absolute encoder. When changing position, the telescope ramps up to a constant velocity and then ramps down as the setting position is approached. Afterward, the telescope backs off about 10° in order to take up any backlash, and then the final setting is made. The telescope can set on a positions in 20 s or less and with an accuracy better than $\pm 10''$, which is more than sufficient considering the large field of view of the FASTT. Furthermore, since the CCD is read out before or while the telescope is setting on the next object, there is no dead time associated with the readout process.

Because the FASTT works without human supervision, safeguards have been implemented for its protection. Inclement weather is the major threat, and a soaking of the telescope could cause serious damage to the electronics located within the telescope enclosure. To prevent this situation, rain sensors (two for redundancy) are located outside of the telescope enclosure and will close the roof if precipitation (rain, sleet, or snow) is detected. A worst-case scenario would be a loss of power prior to the onset of heavy rain, which is a common occurrence during the Arizona monsoon season; and as a result the roof would be unable to close. This possibility is prevented with an auxiliary propane power generator that will automatically come on during a power outage. Hence, there can never be a loss of power. Both the operations of the rain sensors and the power generator are hard-wired in as a further precaution. If they were under software control, then a system crash could cause them to fail to operate properly. Furthermore, the roof of the FASTT enclosure is closed automatically at the end of each night under software control. If the controlling computer were to crash before this final closing, then the roof could be left open during the subsequent day, and as a result the telescope would be exposed to direct sunlight and daytime heating. As a further safety measure, the roof has been placed on a timer (not under software control) that will automatically close the roof at 0700 hours in the morning, if it has not already been closed. Finally, there is usually an observer at the 1.55 m Strand astrometric reflector (located near the FASTT), who is continually monitoring the sky conditions and can manually shut down the FASTT at any time if deemed necessary. This is made possible with a window displayed on the 1.55 m control computer that continually shows the status of the FASTT and is monitored by the observer. Hence, the FASTT has many safety features built into its operation, and because of them the FASTT has successfully operated in automatic mode during the past 10 years without serious mishap.

The quality of the Flagstaff Station observing site is an important factor in determining how much data can be taken with the FASTT. Since the FASTT can observe on every clear night, and downtime is under two to four nights a year, seeing and the weather are the major limitations imposed on the acquisition of data. Characteristics of the Flagstaff observing site are shown in Figure 2. Figure 2*a* shows the relative percentages of time when the sky is clear or workable (defined herein when atmospheric absorption

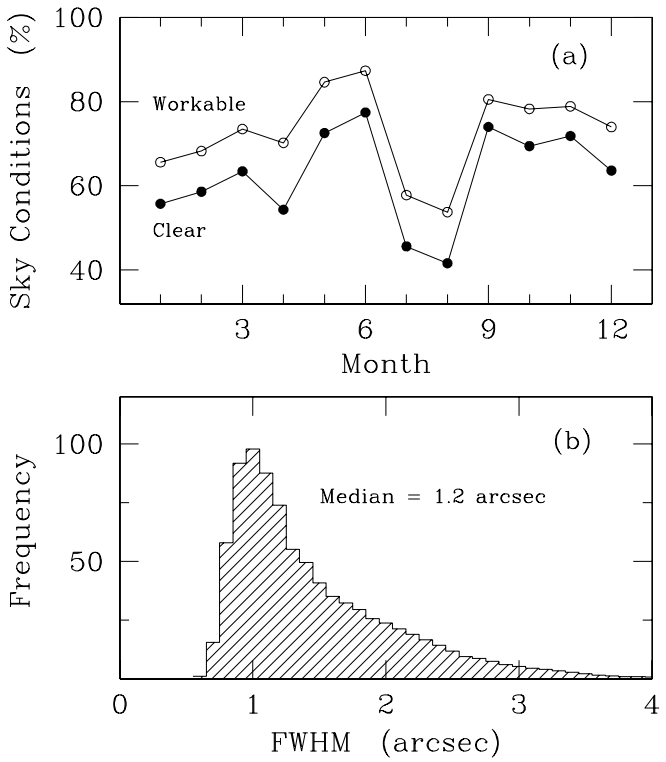

FIG. 2.—Characterizations of the Flagstaff Station observing site, where (*a*) shows average sky transparency and (*b*) seeing as a function of calendar date. In (*a*), "clear" refers to the percentage of clear nighttime hours, while "workable" pertains to conditions with cloud extinctions under 0.75 mag (considered workable with the FASTT). The dip in July and August is caused by the monsoon season in Arizona.

is under 0.75 mag). On average, Flagstaff observing conditions are good enough to observe 75% of the time, with the clearest weather occurring in May and June and the worst during the July-August monsoon season. Figure 2*b* gives the distribution in the seeing at the site, which has a median value of 1.″2. Both figures demonstrate the Flagstaff site is very good for astronomical observations (albeit not as good as premier sites in Hawaii and Chile); as a result, the loss of FASTT data caused by poor seeing and the weather is only about 25%. Therefore, the FASTT can take on observing projects that require large amounts of data collected over the course of each year.

3. CCD SCAN OBSERVING

Since the FASTT can only observe along the meridian, and its camera has no moving parts other than its shutter, drift scanning is used to gather the data. Normally, the term "drift scanning" refers to parking the telescope in a position and then clocking the charge images of stars across the entire width of the CCD at the diurnal rate. As a matter of definition, this type of scanning will hereafter be referred to as "full" scanning. Each star is observed with essentially the same exposure, which is defined by the field of view of the CCD and by the declination being observed. As discussed in Stone et al. (1996), full scanning at high declinations can cause serious distortions in stellar images. The basic problem is that stars move across the CCD in arcs at different angular speeds, while full scanning allows only for a fixed translational motion in right ascension. Consequently, stellar images can be distorted into crescents at high declinations, rendering them unusable for astrometry. In general, full scanning is only possible up to a critical declination (defined by the field of view of the CCD), and thereafter increasing numbers of images become badly distorted by the scanning process.

Sometimes it is favorable to use a shorter exposure time and to observe at a higher declination. For example, many solar system objects transit at declinations unfavorable for FASTT full-scanning observations. Moreover, FASTT full scanning is not very efficient when observing objects brighter than $V < 17$, because the exposures are long ($\geq$202 s) and each observation requires a similarly long overhead time to ramp up to a constant exposure. This problem can be rectified by using a different type of scanning, hereafter referred to as "partial" scanning, in which the shutter is opened for a specified period of time while clocking the charge images, closed, and then the CCD is read out to disk. The net result is a "scan frame" consisting of a ramp region followed with a constant-exposure region. The ramp region will take up $(E/E_0)\cos\delta \times 100\%$ of the physical area on a CCD, where parameter E is the exposure time, E_0 is the time for a star to transit the CCD on the celestial equator (202 s for the FASTT), and δ is the declination being observed. The main advantage of partial scanning is that different exposure times can be used, and observations can be taken at higher declinations (see Stone et al. 1996 for more details). The downside is that the usable area on the CCD is reduced by the percentage mentioned above. Nonetheless, partial scanning is possible with the FASTT over a wide range of exposure times (10 to 100 s) and at declinations exceeding 80°. Further elaborations on partial and full scanning are presented in the following discussions.

3.1. *Partial Scanning*

For several different exposure times, Figure 3 shows the percentage of area on the Ford-Loral CCD that is in the constant-exposure region. In the FASTT reductions, the ramp region is considered unusable for astrometry because of the of the varying amounts of exposure. As seen, the constant-exposure region increases with the declination, which is expected, since the width of the ramp in right ascension is proportional to cos δ. Image distortions caused by partial scanning at high declination can reduce the amount of usable area further. As mentioned previously, full scanning at high declinations will cause star images to appear as crescents. However, because the partial scanning discussed in this paper uses considerably shorter exposures (10 to 100 s), images will not be distorted into crescents; rather, they will be elongated into line segments.

Obviously, some sort of criterion needs to be applied to eliminate CCD images badly distorted by partial-scan observing. In the FASTT program the ad hoc rule is that images are rejected in both full and partial scanning when the image axial ratio (the ratio of major to minor axis, as defined by the moment method discussed in Stobie 1980) exceeds 2. For example, Figure 4 shows a 100 s FASTT partial scan taken at declination $\delta = 70°$. The badly distorted images have been edited from the diagram using the above criterion, and, as seen, the images usable for astrometry are confined within a circular area. At higher declinations the radius of the circle decreases, while at lower declinations the opposite is true, and in fact the entire nonramp region of the Ford-Loral CCD is usable at declinations $|\delta| < 47°$. Diagrams similar to Figure 4 were produced for differing exposure times and declinations being observed, and for each case the percentage of CCD area usable for astrometry was calculated subject to the image rejection criterion. The

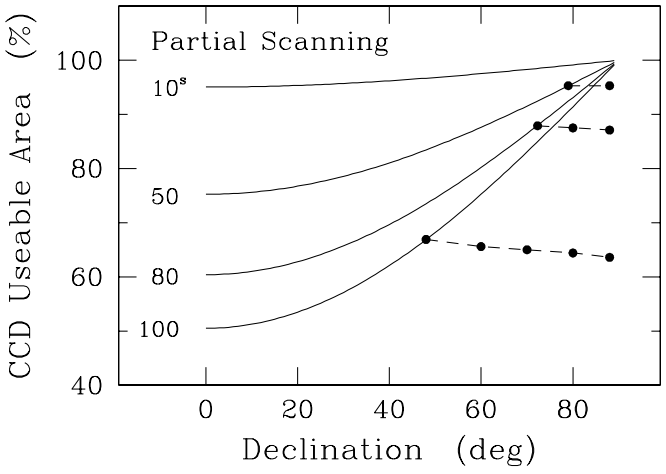

FIG. 3.—In partial scanning, not all of the CCD area is useful for astrometry, and this figure presents results for the Ford-Loral 2048^2 CCD used with the FASTT. The solid curves show the area of constant exposure (or the area exclusive of the ramp-up region) for various declinations and exposure times. The usable area for astrometry is the same as the constant-exposure area at most declinations, but at higher declinations the usable area is reduced further because of image distortions caused by scan observing (see text for details). The dashed curves show the further reductions in the usable area. Clearly, scanning up to the celestial pole is possible with the FASTT, although the usable area of the CCD will be reduced to about 66% for an exposure of 100 s. Greater usable area is available at the shorter exposure times.

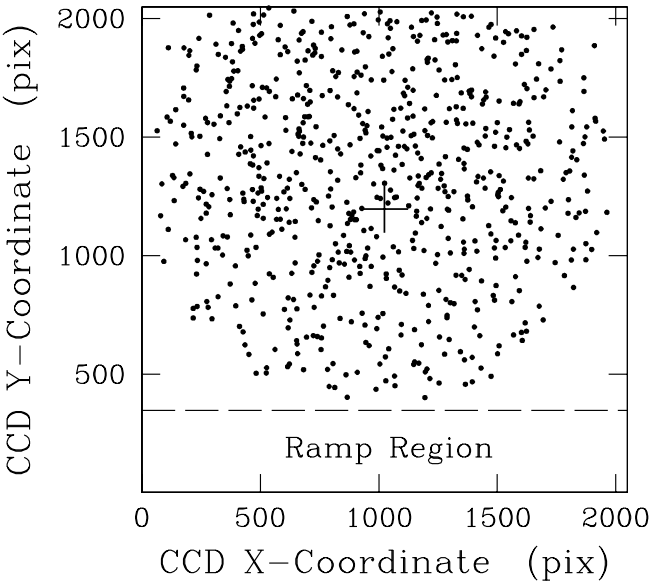

FIG. 4.—Diagram showing the usable area in a FASTT partial scan taken at declination $\delta = 70^\circ$ and with an exposure of 100 s. The ramp and areas with image elongations exceeding 2 (the criterion used in the FASTT reductions to reject badly distorted images) have been excluded. As can be seen, the usable area for astrometry is circular and centered on the constant-exposure area.

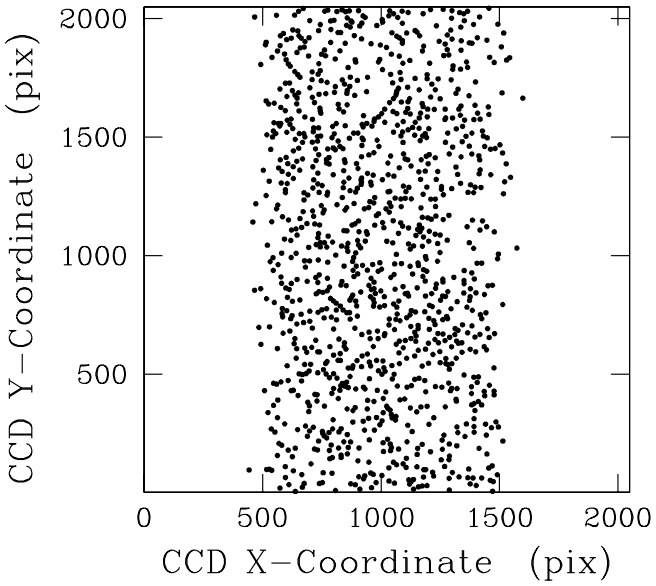

FIG. 5.—Similar to Fig. 4, but showing the usable area associated with FASTT full scanning at a declination of $\delta = 50^\circ$. Away from the equator, image distortions become a serious problem, manifesting themselves first at the top and bottom (northern and southern declination edges) of the CCD, and at high declinations, only good images are found within a narrow band traversing the center of the CCD. For this example, only about 50% of the CCD area is usable because of poor image quality.

results are given in Figure 3, and, as shown, the usable area is the constant-exposure area up to a critical declination, whereupon the area is reduced further by image distortions. The dashed lines in the figure show the further reductions. As also seen from the figure, partial scanning with an exposure time of 100 s is possible almost up to the pole with at least 60% of the CCD area usable for astrometry, over 80% of the area is usable up to the pole with an exposure of 80 s, and all the constant-exposure area is usable up to the pole for exposures under 50 s. Consequently, partial scanning enables the FASTT to observe targets up to the pole that are brighter than $V \sim 17.5$.

3.2. *Full Scanning*

Similar tests were undertaken to explore full scanning. For example, Figure 5 shows images in a FASTT full scan that are usable for astrometry (using the same axial rejection criterion discussed in the previous subsection). The scan was taken at a declination of $\delta = 50^\circ$, and there is no ramp region, since the ramping occurred at the beginning of the exposure and was rejected by the data analysis. The distribution of usable stars is now rectangular instead of circular, which is expected, since in full scanning, all the stars transit the entire width of the CCD in right ascension. The width of the band shown in Figure 5 narrows at higher declinations, and at very high declinations the band is essentially a very thin rectangular box. The usable area of the Ford-Loral CCD was determined empirically at different declinations and is shown graphically in Figure 6. Up to declination $\delta \sim 19^\circ$, the entire area of the CCD is usable for astrometry, and thereafter the band of good images begins to narrow, causing the reduction in the amount of usable area shown in the figure. For scanning along the celestial equator, full scanning is a very efficient means for gathering digital data. This method was used to create the astrometric calibration regions discussed in Stone et al. (1999b), which includes positions and magnitudes for over 1.2 million stars. If at least 50% of the Ford-Loral CCD is to be usable for astrometry while full scanning, then the diagram implies the FASTT can observe only up to a declination of $\delta \sim 40^\circ$. Consequently, many of the targets in FASTT observing programs would be unobservable.

One disadvantage of drift scanning (affecting both full and partial scanning) is that the image point-spread

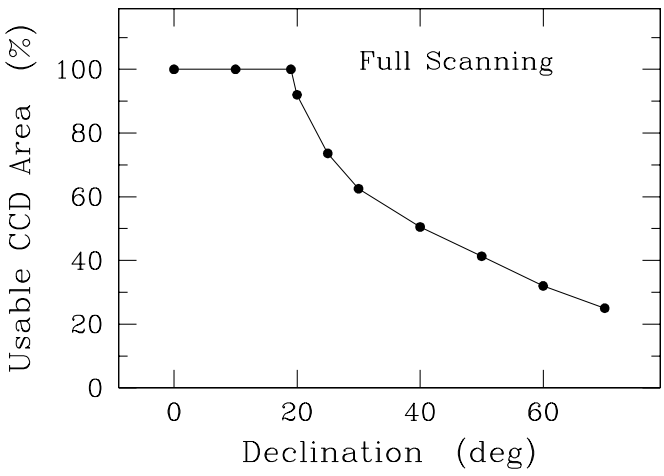

FIG. 6.—At declinations away from the celestial equator, full scanning will be affected increasingly by image distortions caused by the scanning process. This figure shows the usable area of the Ford-Loral CCD, when poor images (elongations greater than 2) have been rejected. Near the equator ($\delta < 19^\circ$), all of the CCD area is useful for astrometry, but at higher declinations, the area decreases and is only 8% at a declination of $\delta = 80^\circ$. Clearly, full scanning is not an efficient method for scanning at high declinations.

function will vary across the CCD because of the distortions described above. As a result, aperture photometry is used with the FASTT (Stone et al. 1996) when determining magnitudes. Moreover, developing a centering routine to closely model scan images would be very complicated and difficult to implement. The use of a conventional centering algorithm can lead to a positional error caused by the inability of the routine to adequately model images altered significantly by scan distortions. In the FASTT program images are centered with a two-dimensional Gaussian fit, and corrections are applied afterward to correct for scan distortions. These corrections were derived from the known characteristics of the Ford-Loral CCD and the geometry affecting the scan observations. Details are given in Stone et al. (1996).

4. AUTOMATED OBSERVING

4.1. *Target Selection*

The selection of targets for each night of FASTT observing is done automatically, taking into account priorities assigned to individual objects and the number of times each has been observed. Input positions for stars are taken from various star catalogs and for solar system objects from the Jet Propulsion Laboratory (JPL) Horizons ephemeris service, discussed by Giorgini et al. (1997). An overall priority is assigned to each object with the following formula:

$$\mathrm{pr} = f_{\mathrm{sky}} f_{\mathrm{gp}} f_{\mathrm{obj}} f_{\mathrm{nobs}} , \qquad (1)$$

wherein each factor is assigned a value ranging from 0 to 1, representing, respectively, lowest and highest priority. Parameter f_{sky} is assigned value 1 if an object is observable during nighttime and secondly is bright enough to observe during the current lunar phase. Otherwise the parameter is set to zero. Nighttime is defined as the time between the end of evening twilight and the beginning of morning twilight, which has been established empirically at Flagstaff and, by definition, is the time when the Sun is 12° below the horizon. It is very difficult to observe faint objects ($V > 15$) near the Moon with the FASTT, and in most cases trying to do so would be a waste of time. As a result, some sort of criterion was needed to indicate when a FASTT observation was possible during bright time. Krisciunas & Schaefer (1991) give formulae to calculate sky brightness caused by the phase of the Moon. These formulae need positions for the Sun and Moon at the time of each observation, and these positions are computed with the analytic equations given by Duffett-Smith (1981). By combining Krisciunas & Schaefer's theory for lunar sky brightness and FASTT empirical data of sky brightnesses, a relation giving the limiting magnitude (for FASTT signal-to-noise detections of $S/N > 7$) as a function of sky brightness was established. This relation is used to reject targets on nights when the Moon is a serious problem. Consequently, only relatively bright objects ($V < 15$) are picked near the Moon. As an illustration, Figure 7 shows objects picked on a night when the Moon rose shortly after the end of evening twilight. The dashed line in the plot gives the limiting magnitude based on the above formalism. As seen, six targets could be observed during dark time (before lunar rise) and many others thereafter, subject to their angular distances from the Moon. The formalism works extremely well in that no targets are lost because of sky noise produced by the Moon.

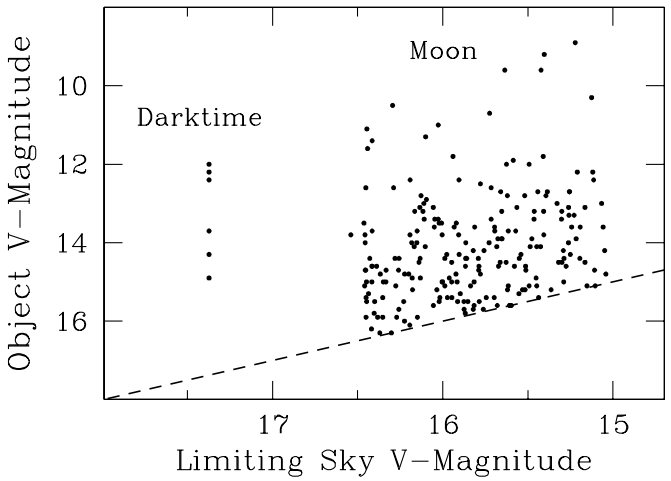

FIG. 7.—The FASTT selects objects for nightly observation according to their brightnesses and the prevailing sky conditions, wherein objects are only picked if the expected S/N of the observation exceeds 7. A model is used to predict the sky brightness that includes the contribution made by the Moon. The figure shows the pick for a night when the Moon rose shortly after nightfall. No objects were chosen below the dashed threshold line, since their images would have been swamped by sky noise. This method of selection is needed in automating observing in order to maximize the number of observations taken in the course of a night.

Second, targets are sorted into groups (sharing common characteristics), and a priority f_{gp} is assigned to each group. For example, planets and planetary satellites are assigned to one group and asteroids intended for mass studies to another. Within each group, secondary priorities f_{obj} are assigned to individual objects, which allows some group members to be observed more often than others. Consequently, the highest priority members of a group will be scheduled for observation first. As a general rule, the priority of an object is reduced each time it is successfully observed so that other objects with a similar priority, but fewer observations, can be observed instead. This is controlled with the f_{nobs} factor given in equation (1). Furthermore, after a group member has been observed a specified number of times within a chosen time window extending backward in time from the current date (e.g., 60 days chosen for asteroids), its assigned f_{nobs} priority is reduced very significantly, thereby giving many other lower priority objects conflicting in time with the given object a chance to be observed. Consequently, the f_{nobs} priority scheme described above is tailored to get a certain number of observations for each group member within the time window associated with the group. This scheme was chosen for solar system objects so that the FASTT would produce a good time line of observations extending over many years. For stars, parameter f_{nobs} is assigned value zero after the formal error in the position has been reduced to under ±10 mas in both coordinates.

Sometimes it is useful to override the priority system described above. For example, if an object has been observed only once within the observing window and a cosmic ray happened to fall near its image, the derived position for the object could be compromised. A second observation taken near the first could identify such an occurrence. In the FASTT observing program an object with only a single observation within the time window is assigned priority $\mathrm{pr} = 1.5$, superseding the priorities given by equation (1) so

that a second observation will be quickly taken. Thereafter, the priority scheme given by equation (1) is reimposed. Hence, the FASTT system favors two or more observations taken at each epoch, which is important for statistical reasons. Secondly, some targets need to be observed on every possible occasion in order to support special projects. An example would be an object scheduled for a spacecraft encounter (the FASTT is currently observing comet Wild-2 for the *Stardust* mission), because navigating the spacecraft to the object depends critically on the ground-based astrometry leading up to the event. Consequently, the priorities for special objects are set to pr = 2.0, which is the highest possible assigned priority and guarantees that an object will be scheduled for observation during every available night. Finally, sometime planetary satellites fall so close to their parent planet that observations taken with the FASTT become impossible. In this case, the satellite is assigned priority pr = 0 so that another object can be scheduled in its place.

After a priority has been assigned to each object, a list is prepared for each night of observation by assigning time slots in the observing queue, starting with the highest and proceeding to the lowest priority object. If two objects with the same priority are competing for the same time slot, then the choice is made in random fashion in order to assure that every object gets an equal chance for observation. Also, an exposure time is assigned to each object according to its predicted magnitude. The goal is to get a good detection ($S/N > 7$), and the adopted exposure times used with the FASTT are listed in Table 2. Furthermore, a model taking into account the individual exposures times and the setting time of the telescope is used to produce a list of objects that the FASTT can observe sequentially in the course of each night. Sometimes there are not enough reference stars within a projected CCD frame, or a target object falls outside of the polygon defining the locations of the accompanying reference stars. Both of these situations can cause serious astrometric errors. As a remedy, the model will shift the center of an observation by as much as 25% of a CCD dimension in either coordinate, looking for a better reference frame, if a problem is expected to occur. These situations arose sometimes when the ACT star catalog was used in making the FASTT reductions. Fortunately, it has been superseded by the much denser Tycho-2 reference star catalog. Moreover, the model will limit the nightly observations to brighter than a specified limiting magnitude. This procedure is useful when the sky conditions are affected by thick cirrus clouds, and only the brightest objects in the observing program can be observed.

TABLE 2
FASTT Exposure Times

V Magnitude	Type of Scanning	Exposure (s)
<14.05	Partial	10
14.05–14.80	Partial	20
14.80–15.20	Partial	30
15.20–15.55	Partial	40
15.55–15.80	Partial	50
15.80–16.00	Partial	60
16.00–17.30	Partial	100
10.50–17.70	Full	202

Because the FASTT is a transit telescope, data can be taken only near the meridian, and in most cases, an object is observed only once in the course of a night. However, exceptions to this rule are the planets Saturn and Uranus, which are each observed twice each night. This is accomplished by using two exposures that are offset respectively in time to the east and west sides of the meridian. The Ford-Loral CCD has a dynamic range of only about 7.3 mag, meaning a single observation would not be sufficient to observe simultaneously both Uranus and its satellites or, secondly, Titan and fainter satellites of Saturn. A short exposure is used to image Uranus or Titan followed with a longer one for the fainter satellites. Consequently, both planets and satellites can be observed each night, notwithstanding the large difference among their magnitudes.

At the end of each night the new observations are tallied with the older ones, and new priorities are assigned to individual objects according to the above procedures. Thereafter, a new list of targets is picked for the following night. This entire process has been automated. One danger with an automated system is that a pathological bad target can be scheduled for every night of operation, meaning not only will the object in question be continually missed, but other important objects conflicting in time will be missed as well. A good example of this would be an object that is too faint to observe with the FASTT, while its published magnitude indicates otherwise. As part of the nightly tallying process the number of times a target has been missed consecutively are recorded as well, and if a target has been missed more than five straight times, then it is flagged for further investigation and, if warranted, removed from the observing queue.

4.2. *Taking the Observations*

The FASTT begins observing at the end of evening twilight and continues until the beginning of morning twilight, as permitted by the weather. In some cases bright targets with very high priorities are observed up to 20 minutes into twilight in order to secure additional observations of them. As mentioned in the previous section, an observing list is prepared for each night of operation, and in the course of the night the FASTT observes sequentially each object on the list. The sequence of operation is the following: the telescope drives and sets on a field, takes the CCD data at the appropriate time, and then drives and sets on the next field while the CCD is read out to disk. Moreover, a series of flats are taken at the end of each night, which are needed in the reductions for positions and magnitudes. In manual observing the observer goes home often after experiencing bad weather for several hours. If it should happen to clear up later, then that data are lost. In contrast, the FASTT will continue to observe throughout the night, regardless of the transparency conditions, and as a result there will be no corresponding loss of data. The operation of the telescope will be curtailed only in the event, or strong likelihood, of precipitation. The frames taken during heavy cloud cover can be easily edited in the reductions, since they will contain few, if any, stars. Even with several magnitudes of extinction, bright objects can be still successfully observed with the FASTT. Concerning productivity, about 22 fields are observed each hour on clear nights, and over 41,000 CCD frames of data are taken during each year of operation.

Much of the early FASTT observing was in full scanning, wherein large areas of the sky were surveyed for star positions, which produced many thousands of positions (see, e.g., Stone et al. 1999b). However, as discussed in § 3, telescopes that use full-scan observing are not well suited for determining positions away from the celestial equator. Currently, the 20 cm USNO CCD Astrograph Catalog (UCAC) equatorial telescope described by Zacharias et al. (2000) is surveying the sky very successfully, and there is little need for the FASTT to reproduce that effort. Rather, the FASTT is primarily concerned with determining highly accurate positions of solar system objects, an area given little importance in modern astrometry. Most objects are observed with partial scanning, but sometimes full scanning is used for high-priority objects that are situated within 35° of the celestial equator.

4.3. *Reduction for Positions and Magnitudes*

After each night of observation the raw CCD data along with ancillary environmental readings (ambient temperatures, pressures, and dew points) are reduced automatically to final ICRS equatorial coordinates and magnitudes and then collated with other existing observations. The process begins at the end of each night, whereupon all the stored CCD frames are flattened using the flat frames taken during the night. The flattening differs from that associated with traditional stare observing. In stare observing the position of an object remains essentially at the same pixel location throughout the exposure. This is not true for scan observing, where there is a starting and ending pixel location corresponding to the beginning and ending times of the exposure. As a result, each CCD scan frame is flattened by taking a normal stare flat frame and integrating along its columns by a length equal to that of the ramp expressed in pixel units. Moreover, the FASTT does not discriminate between clear and cloudy conditions, that is, CCD frames are taken in both cases. The data are later edited in software, where frames are rejected if they contain few or no star images. Otherwise, targets and reference stars in the flattened CCD frames are reduced to final positions and magnitudes with the following procedures.

4.3.1. *Image Processing*

Individual objects present in each CCD frame are identified using a local maximum search and centered with a two-dimensional Gaussian algorithm given by the following standard equation:

$$I(x,y) = b + I_o \exp\left[-\frac{1}{2}\left(\frac{x-x_c}{\sigma_x}\right)^2\right] \times \exp\left[-\frac{1}{2}\left(\frac{y-y_c}{\sigma_y}\right)^2\right], \quad (2)$$

where $I(x, y)$ is the DN count at pixel location (x, y) and b, I_o, x_c, y_c, σ_x, and σ_y are, respectively, the background level, the height of the image, the centroid in x and y, and the dispersions in the x- and y-coordinate directions. The equation is highly nonlinear and must be solved using iterative solutions. Initial values for the above parameters are assumed and refined with least-squares adjustments, and convergence is rapid and usually occurs in two to three iterations. Positions are rejected for a number of reasons, such as being very elongated (axial ratios exceeding 2), being blended with a nearby star, or being saturated. Many of the rejected images involve nearby cosmic-ray hits, which is a problem when using a large-format CCD and long exposure times. Nonetheless, those images can be easily identified and eliminated because of their unusual point-spread functions. If an image is acceptable, then it is centered, and a string of image parameters is saved for future processing and reference (i.e., x and y center, FWHM in x and y, counts in image, S/N, roundness, image height, and sky background level). As discussed in Stone & Harris (2000), centering routines assuming a flat sky background can produce very large (>0.″5) centering errors when applied to satellites located near bright planets. For example, Figure 8*a* shows Triton badly sloped by the glare produced by nearby Neptune. In the FASTT reductions (see Stone & Harris 2000 for details) the nonuniform background caused by the glare of a planet is removed (Fig. 8*b*) before the centering process is performed, thereby removing this source of astrometric error.

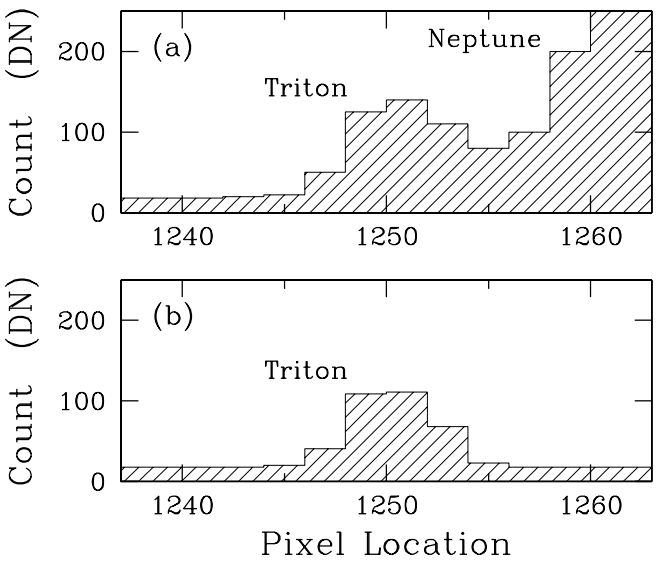

FIG. 8.—Most image centering algorithms assume a flat sky background. When observing satellites near a bright planet (many satellites of planets from Jupiter to Neptune fall into this category), the glare of the planet will cause a steep gradient in the sky level that can, in turn, adversely bias the centroid for a satellite. In the FASTT program, images are corrected for variable background levels, before a two-dimensional Gaussian fit is used to determine their image centers. (*a*) Cross-sectional view of a FASTT image of Triton strongly affected by the glare of nearby Neptune. (*b*) The same image after the sky has been flattened. Without the flattening process, the error in the center for Triton would have exceeded 0.″5.

4.3.2. *Differential Reductions for Positions*

This process begins by finding the Tycho-2 (Høg et al. 2000) reference stars present in each CCD frame of data. Only Tycho-2 stars with more than one positional determination and having proper motions are used in the FASTT reductions (These stars can be identified from the flags given in the Tycho-2 star catalog). First, the expected Tycho-2 stars present in each frame are identified from their coordinates and the known pointing of the telescope. The closest possible match between catalog and observed coordinates is made by applying corrections to convert Tycho-2 coordinates to apparent places and correcting the CCD coordinates for atmospheric refraction, scan distortions, known focal-plane errors, magnitude-related errors, and

diurnal aberration. Next, the brightest 50 stars in each frame are found using a rapid search looking for stars with large image heights. The CCD coordinates of these stars are then converted to pseudostandard coordinates and then compared with the known standard coordinates of the reference stars. The catalog and CCD patterns of stars are matched, assuming initially only offsets in each coordinate direction. This is achieved by searching for a large number of stars sharing a common set of coordinate spacings. When fields are located at low Galactic latitude, it is very important that a large number of coincident pairings be used because of the potential for many false detections. Most stars can be matched using the simple offset model. However, others can be missed if the CCD is tilted with respect to the sky. A finer matching process is then used, whereby the initial matchings are used with standard least-squares reductions, allowing for changes in zero point, scale, and orientation to find all the matchings.

After each Tycho-2 star is paired with its corresponding CCD coordinates, the following equations allowing for changes in zero point, orientation, and scale are derived using standard least-squares solutions:

$$x - X = c_1 + c_2 x + c_3 y \,, \tag{3}$$

$$y - Y = c'_1 + c'_2 x + c'_3 y \,, \tag{4}$$

which relate CCD (x, y) and (X, Y) standard coordinates for the Tycho-2 stars present in each CCD frame. Figure 9 shows the average number of Tycho-2 stars expected in each FASTT frame as a function of Galactic latitude. As can be seen, the number of stars decreases when going away from the Galactic plane, and near the Galactic pole, only about 14 stars are expected in each frame. Nonetheless, there are enough Tycho-2 stars to accurately determine the coefficient in equations (3) and (4) even near the Galactic pole. This was not always the case, when the ACT star catalog (Urban, Corbin, & Wycoff 1998) was used to reduce the FASTT data. Fortunately, the Tycho-2 Catalogue became available in 2000 and contains about 2.5 times more stars than in the ACT. When residuals from the above equations are plotted against (x, y) coordinates, magnitude, and coma, there is no evidence of higher order terms; hence, the simple three-parameter model is sufficient for the FASTT reductions.

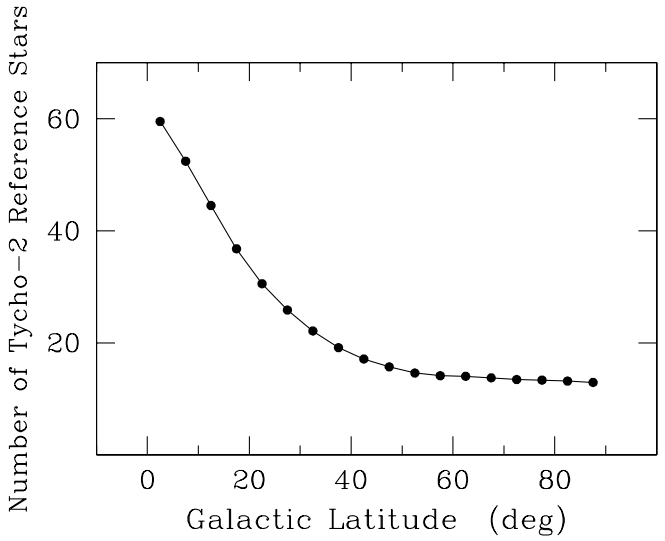

FIG. 9.—Average number of Tycho-2 reference stars present in a FASTT CCD frame as a function of Galactic latitude. The increase in the number of available stars with Galactic latitude is expected, since Tycho-2 is largely a magnitude-limited catalog. At all Galactic latitudes, there are enough reference stars for the FASTT reductions described in § 4.3.2. This might not be true for a CCD with a smaller field of view.

TABLE 3
TYCHO-2 STAR WEIGHTING FACTORS

V Magnitude	Weight	Tycho-2 Stars	Tycho-2 Error (mas)
<11	1.00	864,345	±27
11–12	0.50	1,127,627	±71
>12	0.25	547,935	±104

In order to achieve the best overall accuracy, the above reductions should allow for the widely differing accuracies of Tycho-2 stars. In the FASTT reductions each reference star is weighted according to the scheme given in Table 3, based on their formal errors given in the Tycho-2 Catalogue. The weighting is important, since stars brighter than $V < 11$ are considerably more accurate than those at the faint end of the Tycho-2 Catalog ($V > 12$). Moreover, the least-squares reductions are edited in an iterative manner to remove stars with unusually large residuals (more than 3 times the unit error of the fit). If not removed, these stars could seriously distort the least-squares solutions. Finally, after the unknowns in the above equations are well determined, they are used first to compute standard coordinates for all the target objects in each CCD frame using the above equations; and, second, these coordinates are converted to ICRS equatorial coordinates using the standard transformations given in Green (1985, p. 310). Targets are identified as those objects that happen to fall within a search box centered on their expected positions. The box dimensions are chosen to be $5'' \times 5''$ for stars and $10'' \times 10''$ for asteroids and comets (sometimes a much larger box is used when a particular ephemeris is known to have very large errors). If two or more objects fall within the search box (a problem mostly at low Galactic latitudes), then all candidates are retained, and spurious identifications are rejected later during the editing process (see § 4.5 for details). As an addendum, the derived positions of solar system objects are corrected for phase effects and, as an option, given either as topocentric or geocentric coordinates (see Stone & Harris 2000 for the details). Finally, all the observed and intermediate data (e.g., pixel locations, reference-star ICRS positions, derived positions, and magnitudes) are saved so that the data for any object can be rereduced in the future, if, for example, a better reference star catalog should become available.

4.3.3. *Reduction for Magnitudes*

Accurate magnitudes are computed for all FASTT observations of stars and solar system objects. Standard reductions are used, whereby the count rate (CR) for an object can be converted into a Johnson V magnitude using the following relation:

$$V = \zeta - k_1 X - 2.5 \log \mathrm{CR} + \epsilon_v (B-V) \,, \tag{5}$$

where ζ is a zero-point offset, k_1 is the primary extinction coefficient, X is the air mass being observed, $B-V$ is the

color of the object, and ϵ_v is the instrumental transformation coefficient. Parameters k_1 (seasonally adjusted values) and ϵ_v ($\epsilon_v = 0.363 \pm 0.003$ [s.e.]) have been determined in the usual fashion utilizing observations of *UBV* photometric standards taken from Landolt (1983, 1992) and Graham (1982). $B-V$ colors are given in the Tycho-2 Catalogue for the reference stars; however, colors are not available for many observed asteroids, comets, and stars fainter than the Tycho-2 Catalogue magnitude limit. For these objects, representative colors of $B-V = 0.8$ for asteroids and comets and $B-V = 0.7$ for stars are assumed and used in the reductions. With the above parameters known, least-squares reductions are used then to derive the ζ zero-point offset using the Tycho-2 stars present in each CCD frame, whereupon equation (5) is used to determine magnitudes for all objects identified in each CCD frame. Tycho-2 stars flagged in the catalog as variables or having poor photometry are not used in these reductions. The magnitude of an object with unknown color can be converted later into a true magnitude, if its true color should eventually become known. This is achieved by adding to the approximate magnitude (computed with the above equation) the additive correction $\Delta V = \epsilon_v(B-V)_{\rm true} - \epsilon_v(B-V)_{\rm approx}$. As will be discussed in § 6, FASTT magnitudes of both stars and asteroids can be used in various research projects.

4.4. *Corrections for Systematic Errors*

The goal of the FASTT observing program is to produce the best possible positions. In particular, extremely good positions are needed for predicting occultation events and providing astrometry for spacecraft missions. Accidental errors can always be beaten down with the taking of more data, but eventually the accuracies achieved will be limited by the systematic errors remaining in the data. As mentioned in § 4.3.2, only three unknowns are used in the FASTT reductions for position. If sources of error cannot be adequately modeling with this simple linear model, then these errors will remain in the data and have a systematic effect. Often in astrometry, additional terms are used in the reductions to improve the level of accuracy. However, this process is not always feasible, for example, when few reference stars are available, or second, when the systematic errors cannot be modeled with polynomial representations. In the FASTT program three sources of systematic error have been identified, calibrated, and removed from the reductions before equations (3) and (4) are applied. These are differential color refraction (DCR), nonlinear focal-plane errors, and magnitude-related errors. These errors are caused, respectively, by atmospheric dispersion, nonlinear distortions in the focal plane, and asymmetric image profiles produced by poor CTE. Each will be discussed in the following subsections.

4.4.1. *Differential Color Refraction*

DCR can be an important source of systematic error, if the color of a target object differs significantly from the mean color of the stellar reference frame used in the reductions. A large color difference, a wide passband, and observations taken at large zenith distances will exacerbate the effect caused by DCR. For example, a star of color $B-V = -0.3$ observed with the FASTT at a zenith distance of ZD = 60° will be displaced 55 mas toward the zenith with respect to a reference frame of mean color $B-V = 0.7$, which is a large error by today's standards and systematic in origin. Discussions of DCR are given in Stone (1984, 1996a, 2002) and by Malyuto & Meinel (2000). As discussed in Stone (2001), the DCR associated with the FASTT has been calibrated as a function of $B-V$ color and observed ZD, based on a large number of comparisons of FASTT observed and Tycho-2 Catalogue star positions. The derived empirical relation is

$$\Delta\delta(\text{arcsec}) = \delta - \delta_{\rm FASTT} = 0.0317[(B-V) - 0.8]\tan \text{ZD}\ , \quad (6)$$

tabulated in Table 4 and shown in Figure 10 along with the theoretical prediction taken from Stone (1984). There is excellent agreement between observation and theory, and, when equation (6) is used as a calibration in the reductions, there is no evidence of DCR affecting the derived positions.

TABLE 4
DIFFERENTIAL COLOR REFRACTION FOR THE FASTT AT A ZENITH DISTANCE OF 45°

Spectral Type	$B-V$	Observed DCR (mas)	Model DCR (mas)
O	−0.31	29	33
B5	−0.16	24	24
A0	0.00	19	17
F0	0.31	9	10
G0	0.59	0	0
K0	0.82	−7	−8
M0	1.41	−26	−34
M5	1.61	−32	−39

4.4.2. *Focal-Plane Positional Errors*

All telescopes are affected to some degree by systematic errors in the focal plane that cannot be removed using polynomial representations (the normal assumption) in the least-squares reductions. These errors can result from

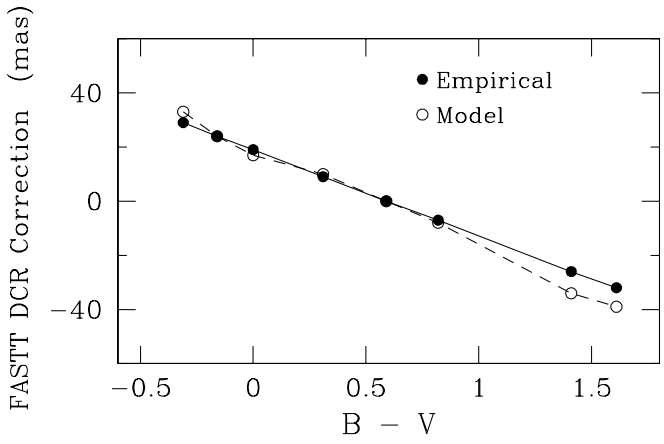

FIG. 10.—As discussed in § 4.4, a correction is applied in the FASTT reductions that allows for differential color refraction (DCR). This source of systematic error can be significant, when the color of a target object differs significantly from the mean color of the reference stars used in the reductions, and when observations are taken at large zenith distances. The FASTT uses an empirically derived calibration which is shown in the plot as a solid line. The theoretical prediction (*dashed line*) is in excellent agreement with the adopted calibration.

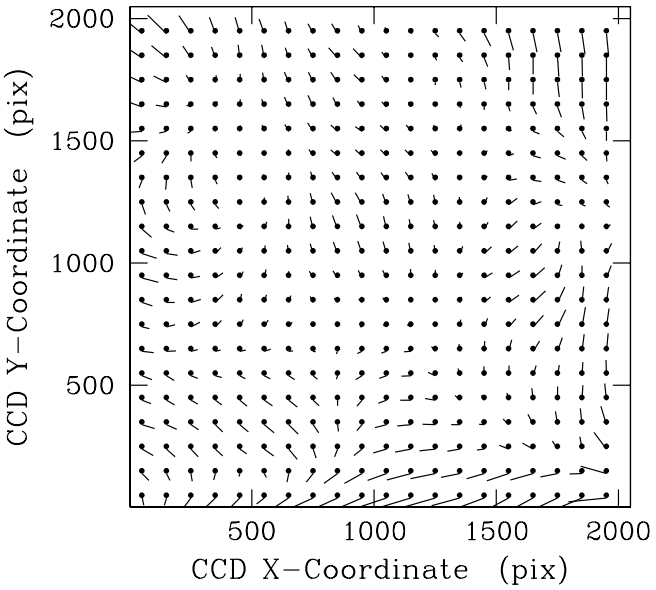

FIG. 11.—Errors exist in the focal plane of the FASTT that cannot be removed with the simple least-squares polynomial fits described in § 4.3. Rather, the errors have been calibrated in terms of Ford-Loral CCD pixel location and are applied in the FASTT reductions as a lookup table. The errors were computed by collating thousands of (FASTT − Tycho-2) differences in coordinate position as a function of pixel position. The figure shows focal-plane errors affecting FASTT positions, characterized by a complicated pattern of swirls. The maximum error is 0.″15.

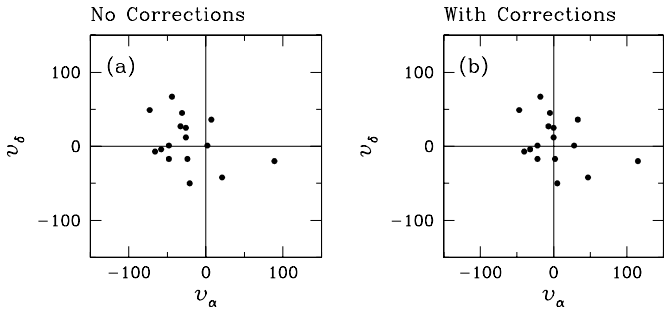

FIG. 12.—Mean (FASTT − Tycho-2) differences in position (v_α, v_δ) for the astrometric calibration stars, respectively, in (*a*) without the focal-plane corrections applied and in (*b*) with their application. The units are in mas. Without the corrections, there is clearly an offset in right ascension, which amounts to 24 mas, a source of systematic error.

distortions caused by the optics, irregularities in the locations of pixels on the CCD, and the mechanical stressing of the CCD. Use of nonlinear terms in the reductions is a complicated process involving iterative least-squares and guesses for the starting parameters. The problem is complicated further when the errors in the focal plane cannot be modeled even with nonlinear techniques. In the FASTT reductions systematic errors in the focal plane are determined in an empirical manner, wherein a large number of (FASTT − Tycho-2) differences in position (gleaned from thousands of observations taken over many nights with short exposures) are collated in bins in the CCD (x, y) focal plane and means formed over the chosen grid pattern. Figure 11 shows the resulting errors in the FASTT focal plane characterized by many whirls and errors that can be as large as 150 mas. In the FASTT reductions, the errors shown in Figure 11 are integrated from the starting to the ending pixel location corresponding with the track of each observed object on the CCD, and the resulting averaged error is used then as a correction in the reductions for position.

As expected, application of this correction improves the systematic accuracy of FASTT derived positions. For example, Figure 12*a* shows mean differences in (FASTT − Tycho-2) coordinate position for the astrometric stars discussed in § 4.5.2 before the focal-plane corrections are applied. There is a significant offset in right ascension amounting to $\langle \Delta\alpha(\text{FASTT} - \text{Tycho-2}) \cos\delta \rangle = 24 \pm 10$ (s.e.) mas, which can be explained by the focal-plane errors found at the center of the CCD, where the astrometric stars were observed. Figure 12*b* shows the same data, but reduced using the corrections, and there is an obvious improvement. With the corrections applied, the mean difference in right ascension is now $\langle \Delta\alpha(\text{FASTT} - \text{Tycho-2}) \cos\delta \rangle = -5 \pm 10$ (s.e.) mas, which is no longer significant. Data are being gathered continually on the Tycho-2 reference stars, which enables the focal-plane corrections shown in Figure 11 to be recalibrated on a regular basis. The normal assumption made in astrometry is that this type of calibration is invariant and only needs to be determined once. The FASTT data show it can change with time, and as result, it needs to be continually redetermined.

4.4.3. *Magnitude-related Errors*

CCDs are inherently linear devices, but, nonetheless, they can be affected by a CTE problem, which can cause a positional error that depends on the number of counts in a stellar image and the distance in pixels between a star's location and a readout register. Herein these errors will be referred to as magnitude-related errors (MREs). Classically, CTE problems are caused by a small amount of charge being left behind with every line shift and can occur in either of the readout directions. When the Ford-Loral CCD was first tested, it showed asymmetric stellar profiles in the serial readout direction caused by poor CTE. The problem was reduced very significantly by raising the CCD operating temperature to -49° C, whereupon the images looked very round, with only a small increase in the dark current. Subsequent tests were undertaken to search for any residual MRE. As reported in Stone (2001), a comparison between FASTT and Tycho-2 positions showed no evidence of an MRE in either right ascension or declination. Unfortunately, that analysis was flawed in that only Tycho-2 stars were used, and, accordingly, the range in stellar magnitude was typically only 2 to 3 mag. Because of the large scatter in the observations, a wider range in magnitude would be needed to better define the MRE. As a result, two other investigations were undertaken to establish the MRE for the FASTT.

First, the program discussed in § 4.5.2 was started, wherein bright Tycho-2 stars ($V \sim 9.4$) and faint International Celestial Reference Frame (ICRF) standards ($14.5 < V < 16.6$) are observed routinely with the FASTT. Both categories of objects are known to have very accurate positions, and currently there are about 70 FASTT positions determined for each of them. Accordingly, accidental errors can be reduced to a very small level by computing mean positions. Figures 13*a* and 13*b* show, respectively,

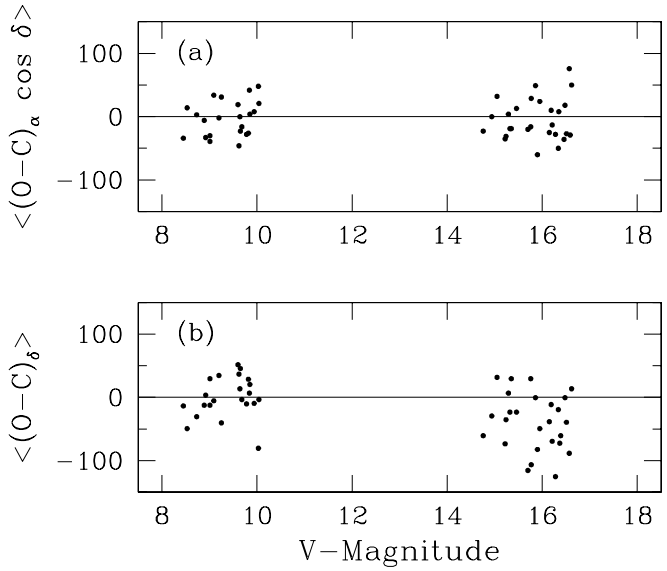

FIG. 13.—Differences in coordinate position (mas) between FASTT and catalog positions of astrometric calibration objects (bright Tycho-2 stars and the optical counterparts of ICRF radio sources), which have been plotted against magnitude. Mean positions are given in order to reduce observational scatter, and clearly, there is evidence for a magnitude-related error affecting FASTT declinations that is removed in the reductions with a calibration.

(FASTT − catalog) differences in position (given in milliarcseconds) for the bright and faint astrometric calibration objects. In right ascension there is no evidence for an MRE; however, there is in declination (serial direction), amounting to 39 mas over the shown range in magnitude. Secondly, FASTT positions of ACR fields (Stone et al. 1999b) were compared with matching data taken with the new US Naval Observatory 1.3 m telescope. Common star fields were observed, and the 1.3 m data were taken in direct and reversed orientations (the camera can be rotated). By averaging the 1.3 m direct and reversed CCD positions, new coordinates independent of any inherent MRE in the 1.3 m CCD can be computed. These, in turn, were compared with the corresponding FASTT data (taken only in the direct orientation, since the FASTT is a scanning instrument) in order to determine any MRE associated with the FASTT. The results were very consistent with the above analysis. An MRE was found only in the serial register direction (declination), which is shown in Figure 14. For comparative purposes, the results derived using the astrometric calibration objects are shown (*crosses*) as well in the figure. There is good agreement between the two independent determinations of MRE in declination for the FASTT. Hence, the MRE in declination is considered well determined and is removed from FASTT data before the reductions for positions discussed in § 4.3.2 are made. Fortunately, this is a simple correction that can be applied retroactively to all FASTT data taken before the correction was determined.

Surprisingly, the MRE in declination for the FASTT does not show a correlation with pixel location, which is expected with classical CTE (i.e., stars closer to the read-out register should be less affected by CTE). The most likely explanation is that the CTE is produced in the summing well of the CCD and, as a result, will only depend on the counts present in each image.

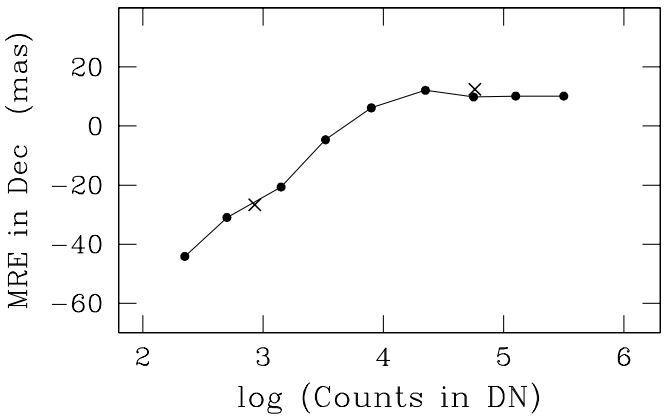

FIG. 14.—Magnitude-related error (MRE) affecting FASTT declinations as a function of counts under the image. The error can be as large as 50 mas, but it is removed in the reductions with a calibration. The two crosses show the MRE based on FASTT observations of astrometric calibration objects.

4.5. *Quality Controls*

4.5.1. *Removing Discordant Observations*

The FASTT produces over 41,000 CCD frames of data each year, and, for various reasons, some of these data will be bad, necessitating the need for a quality control system. One problem concerns the false identification of asteroids. The FASTT searches for asteroids in a $10'' \times 10''$ error box, a size dictated by the expected errors in the ephemerides of these objects. However, by happenstance and particularly a problem in crowded fields, a background star can fall within this search box, causing more than one object to be recorded in a FASTT reduction. Another serious problem occurs when an asteroid moves very close to a background star, producing a blended image. In addition, nights with poor seeing or transparency can produce sometimes bad data as well. The ephemerides for some objects are very poorly known, meaning that it is difficult to detect false identifications on a night-by-night basis. Rather, (FASTT − ephemeris) residuals in coordinate position and magnitude are plotted against calendar date about every 2 weeks for each object in the FASTT observing program, and from these plots erroneous observations resulting from false identifications and other causes can be easily edited, since they stand out from the normal run of residuals. Only about 0.5% of the FASTT observations are rejected by the editing process.

4.5.2. *Astrometric Calibration Objects*

One of the dangers in a large ongoing observing program is that changes in hardware and software might in some way compromise the accuracies of the astrometry being produced. For the FASTT, the hardware and reduction software has been frozen in order to minimize this danger, but sometimes hardware fails and has to be replaced, or the software has to be modified to deal with new projects. In order to monitor the astrometric accuracy of the FASTT, a number of bright Tycho-2 stars with extremely well determined positions and proper motions are observed on a regular basis. Figure 15 shows the distribution of these stars on the sky, which was chosen purposely to give good coverage in both right ascension and declination. In all, there are 24

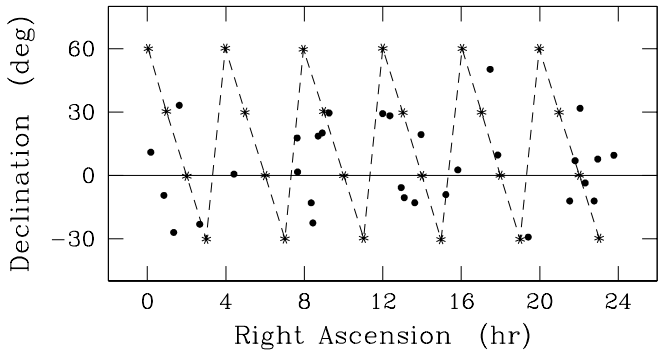

FIG. 15.—Maintaining quality control is important for telescopes that produce huge amounts of data. Changes in hardware or software can inadvertently cause a degradation in the accuracies produced, and if serious enough, a complete loss of data can occur. In the FASTT observing program, observations are taken each night of astrometric calibration objects whose derived positions are used to monitor the astrometric quality of the FASTT on a continual basis. There are two classes of objects. The figure show the bright objects (*asterisks*), which are bright Tycho-2 stars well distributed across the northern sky and a second category consisting of faint ICRF reference sources (*filled circles*) that are observable with the FASTT ($14.5 < V < 16.6$). The second category is used to search for magnitude-dependent errors that could affect FASTT-derived positions.

astrometric calibration stars. Each star is observed about eight times each month, and these data are collated with earlier observations in order to establish a long time baseline of observations. For example, Figure 16 shows (FASTT − Tycho-2) mean differences in position covering the time period 2000.1 to 2002.5, which includes all of the calibration stars. This plot shows the FASTT has been very stable over the specified time period. This conclusion is true also when the stars are broken down into subsets of

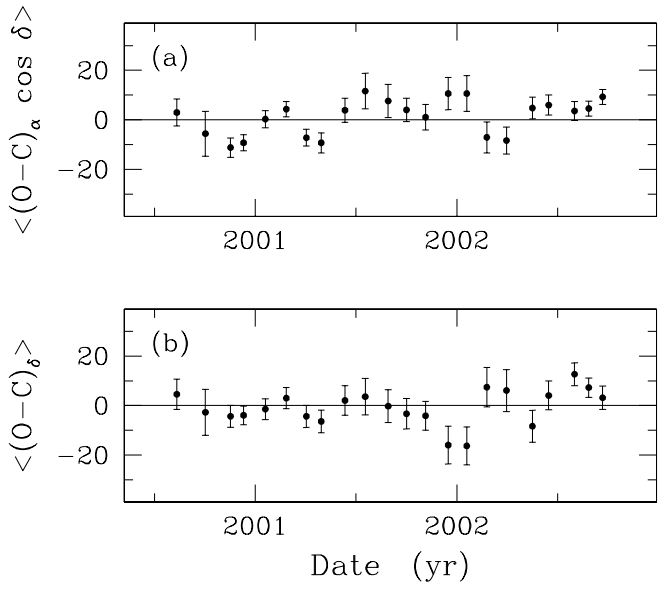

FIG. 16.—Mean differences in position (mas) between FASTT observed and Tycho-2 positions of astrometric calibration stars during the past 2 years of operation. The figures show respectively differences in (*a*) right ascension and (*b*) declination, both of which indicate the quality of FASTT astrometry has been very consistent throughout this period of time. The error bars show 1 σ errors in the differences.

right ascension, declination, and magnitude, although the uncertainties are larger.

Furthermore, the FASTT observes a second set of 31 faint astrometric calibration objects taken from the ICRF catalog (Johnston et al. 1995). These are radio sources generally brighter than $V \leq 16.5$ that do not show appreciable structure in the optical. Most are QSOs, but there are some BL Lacertae objects and galaxies as well. Much like the bright stellar standards discussed in the previous paragraph, these faint sources are distributed across the entire sky, although in a spotty fashion, since the ICRF contains few reference sources. Figure 15 shows the spatial distribution of the faint astrometric calibration objects, which are used to monitor the accuracies of the faintest objects observed with the FASTT. In particular, the FASTT asteroid program includes many faint asteroids ($16 < V < 17.5$), and magnitude-related positional errors can arise from poor CCD charge transfer efficiencies. As discussed in § 4.4.3, observations of faint astrometric calibration objects have provided evidence for a small magnitude-related error in FASTT declinations caused by the charge transfer efficiency of the Ford-Loral CCD used with the FASTT. As discussed in § 4.4.3, this source of error has been calibrated and is removed during the reductions for position.

4.6. *Dissemination of Results*

Within a few hours after each night of observation final positions and magnitudes are computed for all the observed objects and placed then in collated files, so that subsets of data can be easily retrieved using various software programs. As discussed in § 6, many of the FASTT observing programs are time-critical in that positions have to be disseminated to collaborators on very short notice. For example, the chance for successfully observing an occultation depends often on the astrometry obtained in the few days leading up to the event. This can be also true of solar system space missions, where the astrometry just prior to an encounter is used to redirect the spacecraft toward its final approach. Moreover, requests for accurate astrometry to support the radar imaging of near-Earth–passing asteroids are extremely time-critical, since the orbits for these object are often very poorly known and the most important astrometry is needed just prior to the scheduled radar imaging. The FASTT is a very rapid response system, wherein a target can be placed in the observing queue, observed that night, and its position and magnitude sent out the following morning to interested parties. Each subsequent clear night will then produce an additional observation, and in time a considerable database can be produced for individual objects. For projects that are not so time sensitive, FASTT data are made available on timescales ranging from days to months, depending on the needs of individual programs. Positions needed for predicting occultations are usually sent out twice a week, data for planets and planetary satellites on a monthly basis, and all new positions of asteroids about every 3 months to the Minor Planet Center.

5. ACCURACIES ACHIEVED

In this section the accuracies of FASTT observations will be discussed. All observations are affected to some degree by systematic errors (those that cannot be reduced with the taking of more data). As discussed in the above, efforts have

TABLE 5
Error Budget for FASTT Systematic Errors

Error Source	Error in R.A. (mas)	Error in δ (mas)
Uncorrected focal-plane errors	±11	±11
Uncorrected MRE	±10	...
Uncorrected DCR	±8	...
Tycho reference frame	±12	±12
Total	±21	±16

been undertaken to reduce the influence of systematic errors affecting FASTT computed positions. Nonetheless, some systematic error will remain, and the contention of this paper is that this error is caused by small uncertainties remaining in the MRE, focal-plane, and DCR calibrations discussed in § 4.4, as well as an error associated with each reference frame used. Estimates for these uncertainties are presented in Table 5. No errors are listed in the table for the DCR and MRE calibrations in right ascension, since DCR in that coordinate is expected to be insignificant (all observations are taken near the meridian), and no evidence for an MRE in right ascension has ever been found.

Each Tycho-2 star has an error associated with its catalog position that will introduce an error into the reference frame used. The overall error affecting the reference frame can be approximated statistically by computing a mean error for all the reference stars (based on the errors given in the Tycho-2 Catalogue) and then dividing by the square root of the number of reference stars used. If the errors in Table 5 are compounded, then the estimated systematic errors still affecting FASTT right ascensions and declinations are given respectively by the following global values:

$$\sigma_{\rm sys}(\text{R.A.})_{\rm cal} = \pm 21 \text{ mas}\,, \quad \sigma_{\rm sys}(\delta)_{\rm cal} = \pm 16 \text{ mas}\,.$$

The validity of these numbers can be tested observationally using the following analysis: The astrometric calibrations stars discussed in § 4.5.2 were observed repeatedly until the accidental errors in their positions were much smaller than the systematic errors still affecting FASTT star positions. Each star was observed about 80 times, and the resulting scatter in right ascension and declination for these stars is

$$\sigma(\text{R.A.})_{\rm obs} = \pm 28 \text{ mas}\,, \quad \sigma(\delta)_{\rm obs} = \pm 32 \text{ mas}\,.$$

A major source of error in these dispersions is caused by errors in the Tycho-2 Catalogue. The mean catalog error for these stars was found to be ±22 mas in both coordinates, as gleaned from the errors quoted in the Tycho-2 catalog after being carried forward to the mean epoch of each astrometric star observation. When the above dispersions are duly corrected for catalog errors, the following values are found that define statistically the remaining systematic errors still affecting FASTT positions:

$$\sigma_{\rm sys}(\text{R.A.})_{\rm obs} = \pm 17 \text{ mas}\,, \quad \sigma_{\rm sys}(\delta)_{\rm obs} = \pm 23 \text{ mas}\,.$$

These are in excellent agreement with the values calculated above based on the entries given in Table 5. Predicting an occultation event provides a crucial test of the true accuracy of an astrometric telescope. If the astrometry is in error by more than 50 mas, then the event will be missed in most cases. Postanalysis of many occultation events that used FASTT astrometry to make the predictions indicates accuracies of ±30 mas or better.

TABLE 6
Standard Errors in Milliarcseconds of FASTT Positions in Right Ascension and Declination for a Single Observation

	Exposure Time				
V	10 s	50 s	100 s	202 s	Program
7.5–8.0	47	...	...	...	47
8.0–8.5	47	...	...	...	47
8.5–9.0	48	...	...	...	48
9.0–9.5	50	37	...	...	50
9.5–10.0	52	37	...	...	52
10.0–10.5	53	37	27	...	53
10.5–11.0	56	39	28	...	56
11.0–11.5	60	40	29	28	60
11.5–12.0	64	40	29	30	64
12.0–12.5	70	42	31	31	70
12.5–13.0	75	43	33	31	75
13.0–13.5	81	44	33	31	81
13.5–14.0	101	45	33	32	101
14.0–14.5	134	51	36	34	109
14.5–15.0	192	62	44	39	113
15.0–15.5	285	81	56	48	115
15.5–16.0	420	115	72	63	117
16.0–16.5	...	163	103	91	121
16.5–17.0	...	245	147	125	147
17.0–17.5	...	351	217	179	217
17.5–18.0	...	...	301	251	301

The overall accuracy of an individual FASTT observation is given by its accidental error (obtainable from repeated observations of overlapping star fields) and the systematic errors affecting the system. When the accidental error is added in quadrature with the systematic error, the true error of an observation is determined. Following this approach, Table 6 gives FASTT true errors as a function of magnitude for various exposure times. Exposure times 10, 50, and 100 s pertain to partial scans, while 202 s is the time associated with full scanning on the celestial equator with the FASTT. Many different exposure times are used when taking FASTT data, and the last column in the table gives the composite accuracy of the FASTT according to the precepts given in Table 2. Figure 17 shows the results graphically. As expected, longer exposure times give a fainter limiting magnitude and better accuracies for the bright and intermediate-magnitude stars. Of interest, the four curves shown in Figure 17 approach asymptotic limits at their bright end, which is unexpected according to Poisson statistics (see Stone et al. 1996 for details). The likely cause for these limits is the atmosphere. As discussed by Han (1989), turbulence in the atmosphere will produce a positional error defined by

$$\sigma(\text{mas}) = 160(s/10)^{0.32} T^{-1/2}\,, \qquad (7)$$

where parameter s is the spacing in arcminutes between two stars in a CCD frame and T is the exposure time in seconds. The coefficient in the equation will vary with the observing site, and the value given was determined observationally from strip scans taken with the FASTT over many nights. In Table 7 the observed asymptotic limits are given along with expected values computed with equation (7). There is enough agreement between the two sets of numbers to

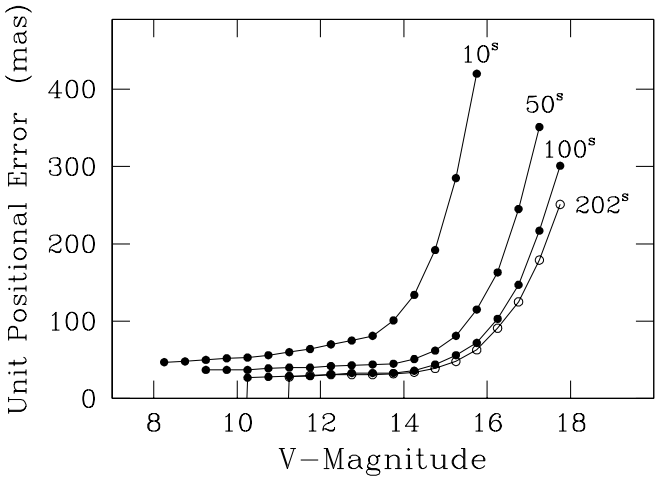

FIG. 17.—Accuracies of FASTT positions (standard errors for a single observation) for four different exposure times. Both FASTT partial (*filled circles*) and full (*open circle*) methods of scanning are shown. As expected, the error increases with magnitude because of lower count rates in the images. In order to make the FASTT observing program efficient and to cover a wide range in magnitude, different exposure times (given by the entries in Table 2) are used in the observational program.

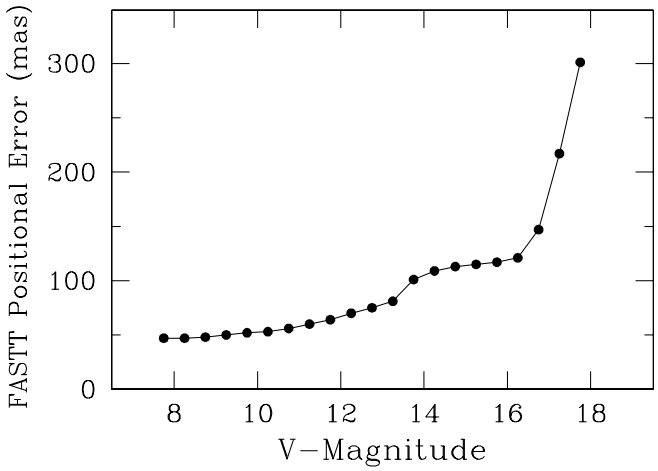

FIG. 18.—Accuracy of FASTT positions for a single observation as a function of apparent magnitude. Only one curve is given, since the accuracies in right ascension and declination are virtually the same. The waviness in the figure is expected, since the FASTT uses different exposure times in the observing program.

believe the asymptotic limits (the accuracies associated the brightest observed FASTT stars) are imposed by the atmosphere, which, in turn, places a hard limit on the accuracies that can be achieved. The sole exception in Table 7 is the 202 s exposure, which corresponds with FASTT full scanning. As discussed in Stone et al. (1996), the atmosphere produces a modulation on the order of minutes that will affect astrometric accuracies. For FASTT exposures under 100 s, this effect will be largely linear and accordingly can be removed with the differential reductions for positions. However, for longer exposures (i.e., FASTT full scanning) this effect can produce quadratic or higher order errors in pixel positions that cannot be removed with the differential reduction model used with the FASTT (see § 4.3.2 for details). Hence, FASTT full scans will be affected by an additional source of systematic error caused by the atmosphere, which probably explains the discrepancy shown in Table 7. According to the table, exposure times of $\geq$100 s are required if accuracies of $\pm$20 mas, or better, are needed for a single observation.

As mentioned earlier, exposure times are assigned to FASTT observations according to the visual magnitudes of target objects. The purpose of this procedure is to give the fainter objects longer exposures and thereby improve their astrometric accuracies. Figure 18 shows the overall accuracy of FASTT positions as a function of apparent magnitude, which is tabulated also in the last column of Table 6. These are the errors expected when a single observation is taken. Since the errors in both right ascension and declination are virtually identical, only one curve is shown. As seen, the FASTT positions are accurate to $\pm$47 mas for bright objects, and at the magnitude limit the accuracy degrades to about $\pm$300 mas. The structure in the curve results from the different exposures used to take the observations.

TABLE 7
ASYMPTOTIC POSITIONAL ERROR

Exposure (s)	Observed (mas)	Model (mas)
10	±44	±47
50	±31	±23
100	±18	±18
202	±20	±10

6. FASTT OBSERVING PROJECTS

Historically, telescopes such as the FASTT were used either to establish a fundamental reference frame of star positions or alternatively densifications thereof. With the release of the *Hipparcos* and Tycho star catalogs (ESA 1997a, 1997b) and subsequent improvements (ACT and Tycho-2 catalogs, described, respectively, by Urban et al. 1998 and Høg et al. 2000), an extremely accurate reference frame, the ICRS, was established, rendering traditional positional astrometry obsolete. As a result, many astrometric telescopes were shut down. However, there is still a niche for small-aperture telescopes that produce large amounts of accurate astrometry and are automated. For one, there is a critical need to extend the ICRS to fainter magnitudes so that large-aperture telescopes will have enough reference stars to use in reductions for star positions. Moreover, the *Hipparcos* mission only provided positions for a handful of solar system objects (planets, planetary satellites, and asteroids) during the brief 3.3 yr time span of the space mission. As a result, there is a critical need for ongoing ground-based observations in order to further improve the ephemerides of solar system objects. Unfortunately, most of the astrometry of solar system objects taken prior to the release of the *Hipparcos* and Tycho catalogs has very poor accuracies (Stone 2000b), and telescopes such as the FASTT offer, in general, a very significant improvement in accuracy. Notwithstanding this need, very few modern astrometric programs devoted to the solar system exist today. Other than the FASTT and the Table Mountain Observatory (Owen, Synnott, & Null 1998), the

vast bulk of solar system astrometry being produced today comes from amateurs using inferior reference-star catalogs.

Starting in 1997, the FASTT began a comprehensive program of observing the outer planets and many of their satellites, thousands of asteroids, and selected comets. Since then, over 170,000 positions have been determined that in many cases have proved crucial in predicting spacecraft encounters with asteroids and observing occultation events. The major FASTT observing programs are described in the following subsections.

6.1. *Solar System Astrometry*

6.1.1. *Planets and Planetary Satellites*

As discussed by Standish (1998), optical observations are critically needed for the outer planetary systems Jupiter to Pluto, since radar ranging and interferometry do not work well at the distances involved. Prior to the release of the *Hipparcos* catalogs, the ephemerides for these planets were largely based on transit-circle observations affected by many sources of systematic error. In particular, the ephemeris for Pluto was in error by several arcseconds. The ephemerides for many of the planetary satellites were also in bad shape. Beginning in 1995, the FASTT undertook a comprehensive program of observing the outer planets Uranus, Neptune, and Pluto in order to establish a long baseline of observations that would include accurate astrometry and extend over many oppositions. Table 8 gives a journal of FASTT observations taken since 1995, which includes over 5600 planetary positions, and the observational program is continuing.

Starting in 1998, the observing program was expanded to include all satellites of Jupiter, Saturn, Uranus, and Neptune accessible to the FASTT. That list now includes the following 17 satellites: Io, Europa, Ganymede, Callisto, Himalia, Elara, and Pasiphae (Jupiter), Tethys, Dione, Rhea, Titan, Hyperion, Iapetus, and Phoebe (Saturn), Titania and Oberon (Uranus), and Triton (Neptune). The FASTT observes the planets Uranus, Neptune, and Pluto and the above satellites on every available night, and currently about 1100 observations of these objects are taken each year. Besides producing a large and homogeneous set of accurate positions, the FASTT data are quickly made available to users and published in a timely fashion. User requests for data can be serviced usually within a manner of hours, and the latter has been achieved with a series of publications (Stone 1996b, 1997b, 1998a, 2000a, 2001; Stone & Harris 2000). Readers are referred to these papers for more details about the FASTT planetary program.

TABLE 8
NUMBER OF FASTT SOLAR SYSTEM OBSERVATIONS

Year	Asteroids	Planets	Planetary Satellites
1995	396	108	...
1996	1196	121	...
1997	1828	195	...
1998	23938	206	865
1999	32011	194	1015
2000	32478	210	827
2001	35158	255	835
2002	37400	233	802

The accuracy of FASTT positions of planets and planetary satellites ranges from ± 80 to ± 250 mas, depending on the apparent magnitude of each observed object (i.e., the astrometry for the fainter objects is degraded because of their lower S/N). As discussed in § 5, efforts were undertaken to improve the accuracies of FASTT positions, and because of these efforts the remaining systematic error in FASTT positions is believed to be only about ± 20 mas in each coordinate. The positions of Uranus, Neptune, and Pluto are determined directly, while those of Jupiter and Saturn are inferred from observations taken of their satellites. Determining an accurate position for Jupiter or Saturn using their disks is very difficult because of their large angular sizes, phase effects, and changing band structures. As pointed out by Morrison & Evans (1998), positions of large Jovian planets are best determined using observations taken of their satellites. Concerning planetary satellites, the vast majority of their positions have been determined historically using differential reductions that placed each satellite in a reference system defined by the ephemeris of its parent planet. In contrast, the FASTT calculates the positions of planetary satellites directly in the ICRS reference frame. More specifically, the FASTT monitors seven satellites each of Jupiter and Saturn, and from these data accurate positions for each planet can be determined. For Uranus and Neptune, their positions can be both determined from direct FASTT observations of each planet and also inferred from FASTT observations taken of their satellites. Hence, two independent sets of positions can be determined for Uranus and Neptune.

FASTT positions of planets and planetary satellites have contributed significantly to recent revisions of JPL ephemerides (Jacobson 2000). For example, Figure 19 gives a bullet diagram showing mean differences in positions

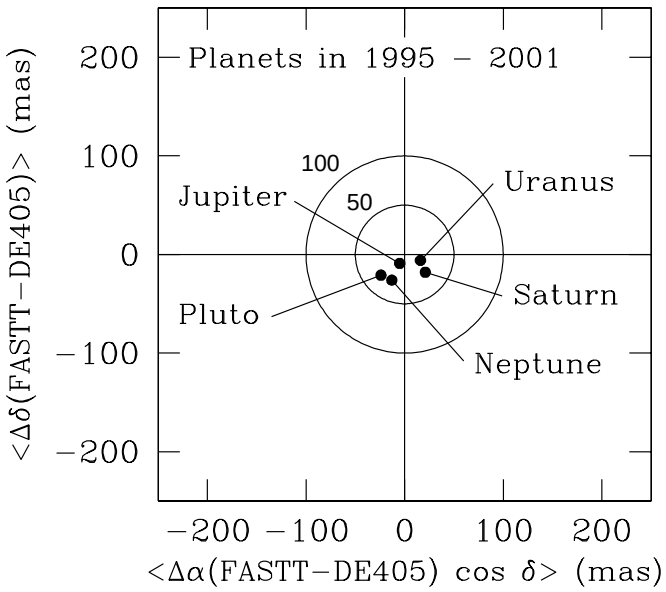

FIG. 19.—Mean differences in position between FASTT observations taken in 1995–2001 of Jupiter, Saturn, Uranus, Neptune, and Pluto and their DE405 predicted positions. The positions for Jupiter and Saturn were derived from FASTT observations taken of many of their satellites. Clearly, there is good agreement between the FASTT data and modern JPL ephemerides for these planets, since all points fall within the 50 mas confidence circle.

between FASTT observations of Jupiter, Saturn, Uranus, Neptune, and Pluto and modern DE405 JPL ephemerides for these planets. As seen, there is good agreement between the FASTT astrometry and the modern ephemerides for each of the planets. The agreement is better than ±30 mas in each coordinate, although there is a hint all of the ephemerides predict declinations that are systematically 16 mas too large. The latter might be caused by the older data used in the production of these ephemerides based on fundamental star catalogs, such as the FK3, FK4, and FK5. Many of these catalogs have a large systematic error in declination (Lindegren et al. 1995). Furthermore, FASTT observations taken of the 17 satellites mentioned above indicate their modern ephemerides are accurate to ±70 mas, or better, in each coordinate, with the exception of Titania and Oberon, satellites of Uranus. FASTT data taken in 1998–2002 show consistently a significant offset in their computed right ascensions amounting to 117 ± 12 (s.e.) mas, which is corroborated by recent observations taken at other observatories.

The FASTT program of observing the outer planets and many of their satellites continues. As mentioned above, there is, in general, good agreement between theory and observation for the planets and satellites included within the FASTT observing program, although this will change in time as the ephemerides age. Figure 20 shows (FASTT − DE405) mean differences in coordinate as a function of date for the planet Pluto. Based on the FASTT data, there appears to be small offsets in the JPL ephemeris for Pluto, amounting to −20 mas in both right ascension and declination, and little evidence of rate changes in either coordinate direction. Consequentially, the current ephemeris for Pluto is quite accurate and should remain so for many years to come. That is certainly not true with the earlier and commonly used DE200 ephemeris for Pluto, which is now obsolete. Concerning the other planets and satellites in the FASTT observing program, none show convincing evidence that their ephemerides are significantly changing with time.

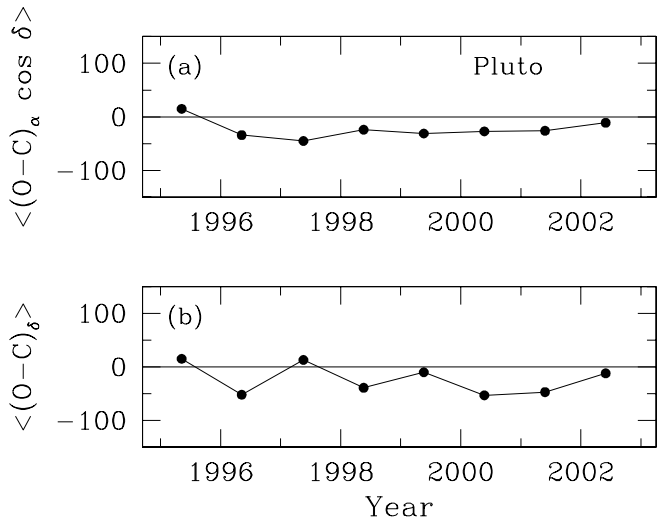

FIG. 20.—Mean (FASTT − DE405 ephemeris) differences in right ascension and declination (mas) for Pluto during the time period 1995 to 2002. As seen, there is good agreement between the two sets of positions (differences under 50 mas typically), despite evidence of small offsets in both coordinate directions. However, there is no evidence that the DE405 ephemeris for Pluto is degrading significantly with time. Hence, it should remain a good ephemeris for many years to come.

Accurate ephemerides for the outer planets and their satellites are needed for various applications, which includes piloting spacecraft to these planets, accurately predicting occultation events, and improving our understanding of the dynamics of these systems. The FASTT has been very involved in all of these aspects, which includes, and has included, providing accurate astrometry to JPL on a monthly basis in support of the *Galileo*, *Cassini*, *Europa Orbiter*, and *Pluto-Kuiper Express* missions to the outer planets. Furthermore, the FASTT has contributed many observations that have significantly helped in predicting recent occultations of Titan, Titania, and Pluto. In particular, the recently observed occultations of P126 and P131.1 by Pluto (McDonald & Elliot 2000) have yielded important new information about the atmosphere of Pluto.

6.1.2. *Asteroids and Comets*

Starting in late 1997, the FASTT commenced a large observational program to observe several thousand asteroids that would extend over a period of years in order to very significantly improve their ephemerides. Except for the very long orbital period asteroids ($P > 6$ yr), each would be observed over a full period so that closure could be reached, ultimately providing extremely good orbits for these objects. Hitherto, the astrometric data for most asteroids consisted of a heterogeneous set of positions afflicted with both large systematic and accidental errors, which in combination can easily exceed ±0.″5 in each coordinate. In contrast, the FASTT program offers typically a tenfold improvement in accuracy and data tied directly into the preferred ICRS reference system. Furthermore, each asteroid in the FASTT program is being observed on a very regular basis (several times each month at least), unlike older data sets, which are often very spotty. The target objects in the FASTT program include the first 2000 numbered asteroids and selected targets for various collaborative research projects. Most of the selected targets are asteroids picked for dynamical mass determinations, asteroids and comets targeted for spacecraft encounters, and asteroids involved in occultation events.

A detailed discussion of the FASTT observational program is given in Stone (2000b), and only highlights of that paper will be reproduced herein. Figure 21 shows the spatial distribution of the asteroids in the FASTT program, and, as seen, the sample includes mostly main-belt objects along with significant numbers of near-Earth, Hilda, and Trojan asteroids. Currently, each of these asteroids has been observed about 80 times, and Figure 22 shows how much of their orbits have been covered so far in the FASTT observing program. As is evident from the figure, the vast majority of the FASTT asteroids have been observed with coverages exceeding 60% of their orbits, and about 25% have more than full-orbit coverage. By the end of 2003 the vast majority of the asteroids in the program will have been observed a full orbit or more. Table 8 gives the number of FASTT observations taken each year of asteroids, and the current total is over 164,000 and is growing at an annual rate of about 37,000 observations per year.

The scientific goals of the FASTT asteroid/comet program are many. By the end of 2003 a very large database for about 2010 asteroids and several comets will become

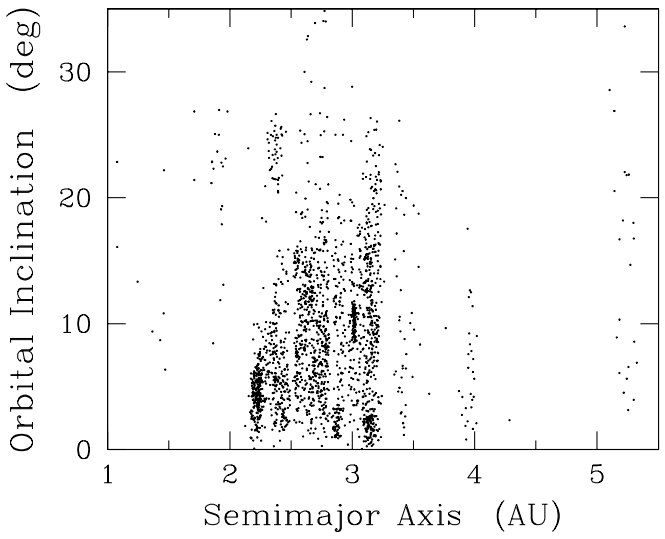

FIG. 21.—Distribution of the asteroids currently being observed with the FASTT in terms of their semimajor axes and orbital inclinations. Most are main-belt objects; however, there are significant samplings of the near-Earth, Hilda, and Trojan asteroids as well.

available that is extremely homogeneous, includes about 190,000 positions, has good time coverage, extends over a full orbital period for most objects, and, finally, consists of highly accurate positions and magnitudes. Support for spacecraft mission has always been given extremely high priority in the FASTT observing program. Starting in 1991, the FASTT contributed astrometry for flybys of the asteroids 951 Gaspra and 243 Ida (Monet et al. 1994) for the *Galileo* mission, 253 Mathilde and 433 Eros for the *NEAR-Shoemaker* mission, and 5535 Annefrank for the *Stardust* mission. Positions were determined also for 1620 Geographos, but, unfortunately, the *Clementine* spacecraft failed before its scheduled encounter with the asteroid. Currently, the FASTT is providing astrometry for the *Stardust* encounter with comet Wild-2 in 2004 January. Furthermore, the FASTT was a major contributor to the success of the New Millennium *Deep Space 1* (*DS1*) mission, wherein FASTT positions of beacon asteroids were used to navigate the spacecraft to the faint asteroid 9969 Braille. The FASTT data in conjunction with the onboard imaging capacity of the spacecraft demonstrated that autonomous navigation with the solar system was possible and most likely will be used in future spacecraft missions. Although Braille was too faint to observe with the FASTT ($V > 18$), the FASTT provided densified reference frames along its path that, in turn, were used with large-aperture telescope data to determine accurate positions for Braille. In fact, the *DS1* spacecraft came within 30 km of the asteroid on closest encounter in 1999 July, but unfortunately the onboard camera failed to image the asteroid.

The FASTT is currently the major contributor of astrometry for predicting occultation events all around the world. Predicting occultations requires extremely accurate positions (often ± 50 mas or better) for any chance of success. Prior to the involvement of FASTT, the astrometry was based largely on differential reductions using the Guide Star Catalog (GSC; described by Russell et al. 1990), which is a catalog with large positional errors, and, accordingly, very few events were actually observed. Figure 23 shows the number of successfully observed occultations since 1975, and, as seen, there is sharp increase starting in 1997 (when the FASTT first started providing data) that now totals over 50 events a year, a sixfold increase since the start of the FASTT involvement. Not only are more events being observed each year (Dunham 2002), but often more chords are being observed with each event, and hence more information is being gleaned about the shapes and sizes of asteroids. Furthermore, the large and growing FASTT database enables more asteroids to be considered for occultation events (in particular, those with fairly small diameters), since good orbits can be now computed for them. Last-minute astrometry, wherein positions for the asteroid and background occultation star are computed in the same CCD frame, is also possible with the FASTT because of its large field of view. Since all the reductions are differential,

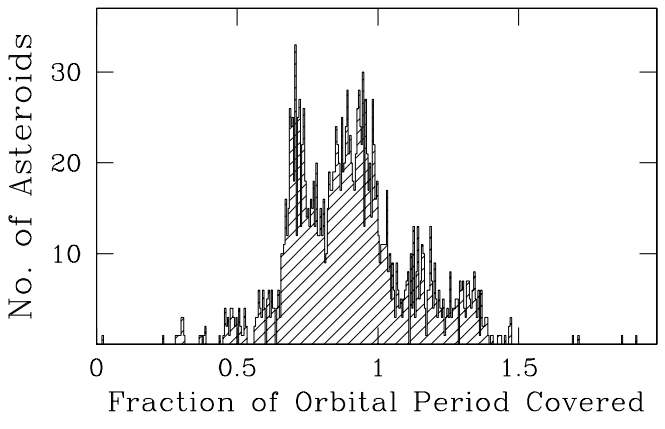

FIG. 22.—The FASTT program to observe asteroids started in earnest in 1997, and this figure gives the current status of the program. In the figure, the asteroids have been sorted according to how much of their orbital periods have been covered with FASTT observations. Currently, the vast majority of the asteroids have been observed with coverage ranging between 60% to 140% of their orbits. The coverage will increase with the taking of more data.

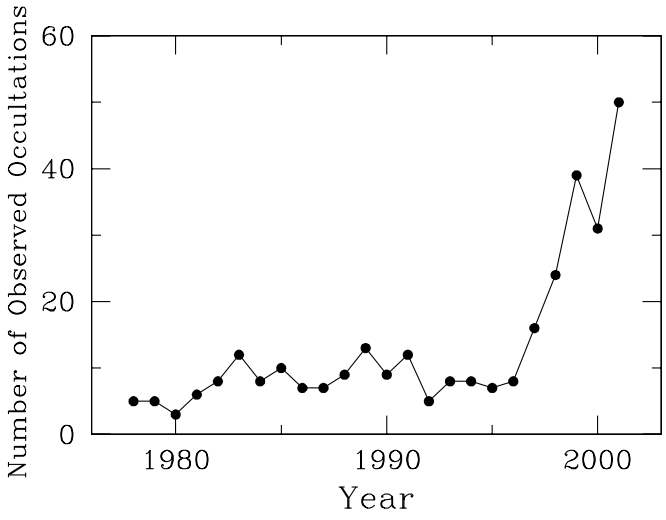

FIG. 23.—Successfully observed occultations involving asteroids as a function of date. The dramatic increase in the number of events starting in 1997 resulted from better predictions based largely on accurate FASTT and Table Mountain Observatory astrometry. The increase is sixfold and increasing with each passing year.

extremely accurate predictions can be make in the last days leading up to an occultation event.

In collaboration with J. Hilton at the US Naval Observatory in Washington FASTT astrometry is being used to significantly improve the orbits of asteroids selected for dynamical mass determinations (Hilton & Stone 1998). The FASTT observes about 15 asteroids each month for this project, and preliminary masses have been computed already for some of the program objects. Masses are known for only a small number of asteroids, and when this particular program is finished, hopefully, many more masses will become available.

FASTT positional data can be used for projects other than those mentioned above. For example, it is being used also to investigate the kinematics of asteroids, look for subgroupings within asteroid families, and aid outside investigations. Concerning the latter, the FASTT receives numerous requests for data in support of various research projects. Among these is astrometry for near-Earth asteroids (NEAs) passing near Earth for radar imaging experiments, of faint cometary nuclei for planned *Hubble Space Telescope* observations, and of asteroids for studying phase effects. As mentioned in § 4.6, the FASTT can respond rapidly to time-critical requests, and often data are available the morning following a request. Otherwise, the bulk of the FASTT asteroid/comet data are made available at the USNO Web site (see instructions in Stone 2000b) and is submitted also to the MPC on a regular basis.

Moreover, during the period 1994 to 1999 the FASTT conducted an observational program in collaboration with Lowell Observatory to improve the ephemerides of NEAs, asteroids with poorly known orbits (to the extent the objects could be lost), and various targets selected by Lowell. Many thousands of observations were taken, which enabled the orbits of the asteroids in the program to be very significantly improved. The reductions were made differentially using either GSC or USNO A-2 star catalogs, and all the results were reported on a timely basis to the MPC for dissemination to the astronomical community. This program is described in Monet (1994, 1995) and in Monet, Bowell, & Monet (1997).

6.2. *Stellar Astrometry*

When the success of the *Hipparcos* satellite was assured, the FASTT observing program largely transitioned to making observations of solar system objects for which there would be a continuing need. Other small-aperture telescopes (Zacharias et al. 2000; Rapaport et al. 2001; Evans, Irwin, & Helmer 2002) have devoted themselves to extending the *Hipparcos*/Tycho-2 catalogs to fainter magnitudes. Concerning the FASTT, a large survey of the northern sky was ruled out, since as discussed in § 3, drift-scan observing can be difficult when observing away from the celestial equator. Moreover, the UCAC pole-to-pole densification program described in Zacharias et al. (2000) is doing the job faster and probably more accurately than the FASTT could ever achieve. Nonetheless, the FASTT was involved in several stellar observing programs. As reported in Stone (1994, 1997c, 1997d, 1998b), FASTT positions were used to verify the link between the *Hipparcos* and ICRS reference frames, as well as to verify the systematic pattern of errors found in the FK5 star catalog (predecessor to the ICRS) by

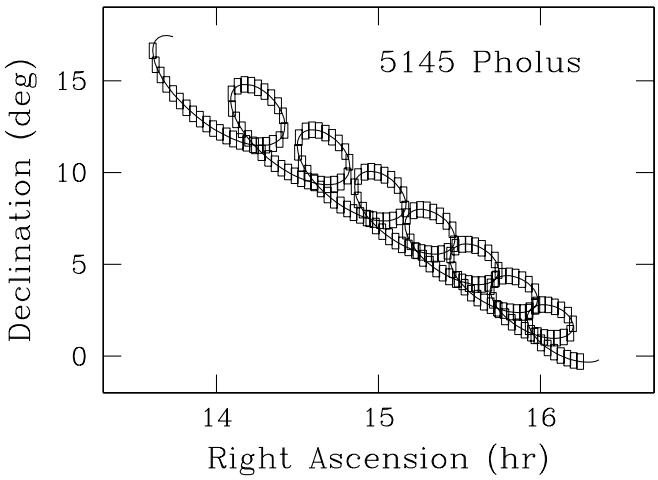

FIG. 24.—An example showing FASTT partial scans taken along the path of the Centaur 5145 Pholus covering the time interval 1999 to 2005. Positions were determined for all the stars in the shown boxes down to a limiting magnitude of $V = 17.7$, and among these, stars were identified that might be occulted by Pholus.

Hipparcos. In both applications *Hipparcos* was found to be an excellent catalog, which is important insofar as it will define the optical reference frame for at least the next decade.

On a much larger scale, the FASTT was used to establish 16 astrometric calibration regions (ACRs) around the celestial equator that extend to fairly deep magnitudes ($V \sim 18$), includes many thousands of stars with accurate positions and magnitudes, and are relatively large (7.°6 by 3.°2) in area. The FASTT observations needed for this project were taken in 1994–1998, and the results were published in Stone (1997e) and in Stone et al. (1999b). The original purpose of this work was to establish calibration fields along the equator that the SDSS telescope could use to calibrate its large focal-plane array of CCD detectors. Many other telescopes use these data today as well. Data for the ACRs are made available at the USNO ftp site (see Stone et al. 1999b for the details) or from major databank centers.

The FASTT was also involved in projects searching for possible occultations involving Centaurs and Kuiper belt objects (KBOs). Included among these were the Centaurs 5145 Pholus and 10199 Chariklo. Densified star positions were determined along the paths of these objects within the 1999–2005 time frame, and among the measured stars, occultation candidates were identified and published, respectively, in Stone, McDonald, & Elliot (1999a) and Stone et al. (2000). As an example, Figure 24 shows the pattern of overlapping partial scans taken with the FASTT to map out the path of Pholus over seven consecutive oppositions. Over 98,000 stars were investigated, and among these, likely occultation candidates were identified. In addition, the FASTT is searching for stars that might be occulted by various KBOs in the coming years.

Finally, the FASTT is being used to provide densified reference frames in small fields that, in combination with large-aperture telescope CCD data, can be used to determine accurate positions for various objects that are too faint to observe with the FASTT. Included among these are faint satellites of planets, as well as various asteroids and comets.

6.3. *Photometry*

Magnitudes are determined with each FASTT observation. The reductions were described in § 4.3.3, and the accuracies achieved are illustrated in Figure 25. As mentioned in § 4.1, exposure times are chosen by apparent magnitude, and because of that procedure, the error curve shown in the figure has a waviness associated with it. Considering the FASTT is only a 20 cm telescope, the derived magnitudes are quite accurate and extend to a relatively faint magnitude, $V \sim 17.5$. The magnitudes are being used for various photometric investigations, and among these, the major ones will be described in the following discussions.

When the FASTT program of observing the first 2000 numbered asteroids matures in 2003, there will about 95 magnitude determinations for each asteroid extending over many oppositions. Unfortunately, asteroid light curves cannot be determined in most cases using only FASTT data, since as a transit telescope, all observations are taken near the meridian, and as a result objects can be observed at most once each night, meaning the minimum spacing between consecutive observations is about 24 sidereal hours. Considering that most asteroids have much shorter periods of rotation, aliasing prevents unambiguous periods to be determined for them using FASTT data alone. Nevertheless, FASTT photometry of asteroids can be used to identify asteroids with large variations in their light curves (as identified by the rms scatter in the FASTT magnitudes), which are probably asteroids with large light amplitudes. Figure 26 shows how these dispersions are distributed for the asteroids included in the FASTT observing program. Most dispersions are under ± 0.15 mag; however, there are a significant number with values exceeding ± 0.25 mag. Follow-up USNO 1 m reflector photometry of asteroids with dispersions $\sigma_V > \pm 0.25$ finds they have indeed large amplitudes and interestingly very similarly shaped light curves, indicating they are most likely rotating bars and cones (see Stone 2000b for more details). Other uses for FASTT magnitudes includes investigating the opposition effect, searching for binary asteroids, determining the shapes of asteroids photometrically, and investigating asteroidal precessional motions. References for these applications are given in Stone (2000b).

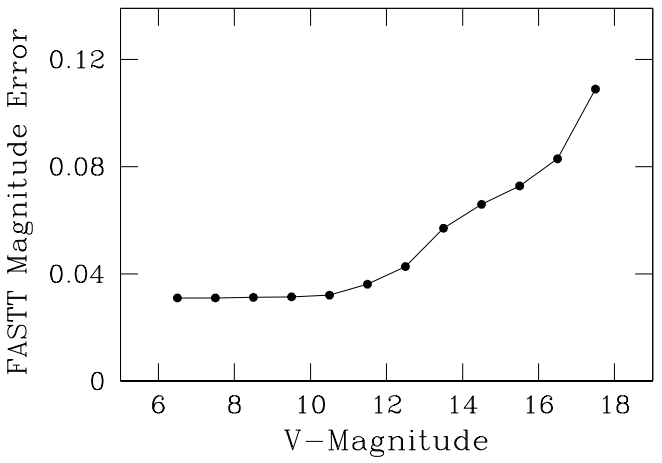

FIG. 25.—Error in a single FASTT magnitude determination as a function of magnitude. The curve has an unusual shape, since not all observations are taken with the same exposure, a policy chosen to increase the efficiency of the observing program (see § 4.1 for details).

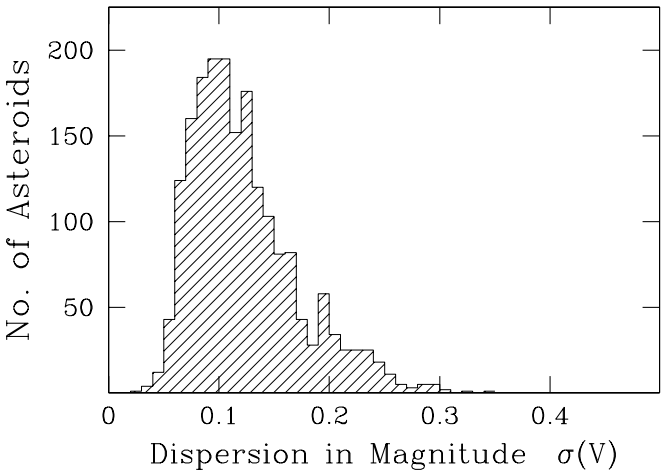

FIG. 26.—Distribution of FASTT asteroids binned by the dispersions in their magnitudes. The dispersions are caused in most cases by rotation and the irregular shapes of individual asteroids. As mentioned in the text, the smaller asteroids show the largest dispersions and presumably are more irregular in shape.

As part of the ACR project described in § 6.2, over 1,268,732 FASTT magnitudes of 661,591 stars were produced and subsequently used to identify variable stars present in the ACRs (Henden & Stone 1998). Over 1600 variables were identified, and 95% of these were new identifications. Although the FASTT is currently not searching for variable stars, this might not be true in the future, since scan observing near the celestial equator would be very productive in identifying new variable stars, as indicated by the ACR work.

7. CONCLUDING REMARKS

Many small-aperture telescopes (<0.5 m) were involved in stellar astrometry prior to the *Hipparcos* mission. However, the great success of that mission has rendered most ground-based astrometric programs obsolete, and accordingly many of those telescopes have been shut down. Nonetheless, there are still niches for small telescope astrometric programs: namely, with their generally large field of views, they can be used to densify the *Hipparcos*/Tycho-2 catalogs to fainter magnitudes or transition to solar system astrometry, an area where the astrometry has to be continually updated with new observations in order to keep the ephemerides current. A number of small telescopes are involved in densification, and in particular, the UCAC program (Zacharias et al. 2000) will provide an extension of *Hipparcos* to $R \sim 16$ with very good accuracies. After its completion in a few years, the UCAC catalog will become the catalog of choice for making astrometric reductions. Further densification will require telescopes of medium to large aperture, and efforts are being taken in that direction at several observatories.

Solar system astrometry has been largely ignored by astrometrists for decades, and as a result, the positions for most objects are quite poorly known and afflicted in most cases by serious systematic errors. For example,

observations with errors under $\sigma \sim \pm 0''.5$ are considered to be of exceptional quality. Accurate astrometry of solar system objects (planets, planetary satellites, asteroids, and comets) has become increasingly important for a number of reasons. For one, accurate positions are needed to update the ephemerides of many objects in support of various spacecraft missions, where ground-based astrometry is critically needed to navigate each spacecraft to its intended target. In particular, the number of spacecraft missions to the outer solar system, asteroids, and comets has increased dramatically over the past decade, and this trend is likely to continue. Moreover, good astrometry is needed to predict occultation events which give critical information about the shapes and sizes of solar system objects, and in some cases, information about their atmospheres and surrounding coma. Predictions better than ± 50 mas are needed often for these events, which is rarely possible with the existing state of solar system astrometry. Modern telescopes equipped with CCD detectors and using differential reductions tied into the Tycho-2 Catalogue can improve very significantly the accuracies of these predictions. For example, the FASTT and Table Mountain Observatory (Owen et al. 1998) observations of asteroids have led to a sixfold increase in the number of successfully observed occultations since 1997, representing a very dramatic improvement. Moreover, good astrometry is needed to determine accurate orbits for newly discovered NEAs, improve the ephemerides of Jupiter, Saturn, Uranus, Neptune, and Pluto (which are still based on optical observations), compute better orbits for planetary satellites (many of which are not well known), identify new families of asteroids, understand the kinematics of comets and other objects, and improve our understanding of gravitational theory.

Small-aperture telescopes can contribute in these areas if they provide copious amounts of accurate astrometry in a very cost-effective manner. Automation and the application of modern astrometric methods provide the means to achieve these objectives. For example, the manpower needs for the FASTT are under one person per year, total operational costs are negligible compared to large telescope operations, and the FASTT produces many thousands of quality observations each year. Future improvements to the FASTT might include the real-time reduction of data and an increase in productivity by using a thinned CCD which would have a significantly greater quantum efficiency (QE) over the thick front-illuminated CCD currently in use as well as better CTE. A higher QE would mean more observations could be taken each night. Other small telescopes can follow suit. Nonetheless, older telescopes, such as the FASTT, have a limited lifetime inasmuch as new highly modern telescopes are being built that will surpass them in terms of productivity and the ability to reach very faint magnitudes. As an example, the USNO has constructed a 1.3 m telescope at Flagstaff (Monet et al. 2001) that will be highly automated, have a large field of view mosaicked with six CCDs, and be able to survey large regions of the sky down to $V \sim 21$ quite rapidly. This telescope will be used for solar system astrometry, among other applications, and can easily surpass the FASTT in terms of overall accuracies achieved and numbers of objects observed each night.

REFERENCES

Duffett-Smith, P. 1981, Practical Astronomy with Your Calculator (2d ed.; Cambridge: Cambridge Univ. Press)
Dunham, D. W. 2002, S&T, 103(3), 92
ESA. 1997a, The Hipparcos and Tycho Catalogues, Vol. 3, (ESA SP-1200) (Noordwijk: ESA)
———. 1997b, The Hipparcos and Tycho Catalogues, Vol. 4, (ESA SP-1200) (Noordwijk: ESA)
Evans, D. W., Irwin, M. J., & Helmer, L. 2002, A&A, 395, 347
Fricke, W., Schwan, H., & Lederle, T. 1988, Veröff. Astron. Rechen-Inst. Heidelberg, No. 32
Giorgini, J. D., et al. 1997, Horizons: JPL's On-Line Solar System Data and Ephemeris Computation Service (Pasadena: JPL)
Graham, J. A. 1982, PASP, 94, 244
Green, R. M. 1985, Spherical Astronomy (Cambridge: Cambridge Univ. Press)
Han, I. 1989, AJ, 97, 607
Henden, A. A., & Stone, R. C. 1998, AJ, 115, 296
Hilton, J. L., & Stone, R. C. 1998, in IAU Colloq. 172, Impact of Modern Dynamics in Astronomy, ed. J. Henrard & S. Ferraz-Mello (Dordrecht: Kluwer), 361
Høg, E., et al. 2000, A&A, 355, L27
Jacobson, R. A. 2000, AJ, 120, 2679
Johnston, K. J., et al. 1995, AJ, 110, 880
Krisciunas, K., & Schaefer, B. E. 1991, PASP, 103, 1033
Landolt, A. U. 1983, AJ, 88, 439
———. 1992, AJ, 104, 340
Lindegren, L., et al. 1995, A&A, 304, 44
Malyuto, V., & Meinel, M. 2000, A&AS, 142, 457
McDonald, S. W., & Elliot, J. L. 2000, AJ, 119, 1999 (erratum 120, 1599)
Monet, A. K. B. 1994, BAAS, 26, 1376
———. 1995, in IAU Symp. 166, Astronomical and Astrophysical Objectives of Sub-Milliarcsecond Optical Astrometry, ed. E. Høg & P. K. Seidelmann (Dordrecht: Kluwer), 405
Monet, A. K. B., Bowell, E., & Monet, D. G. 1997, BAAS, 29, 1273
Monet, A. K. B., Harris, F. H., Harris, H. C., Monet, D. G., & Stone, R. C. 2001, BAAS, 33, Div. Dyn. Astron. abstr. No. 4.04
Monet, A. K. B., et al. 1994, AJ, 107, 2290
Morrison, L. V., & Evans, D. W. 1998, A&AS, 132, 381
Owen, W. M., Jr., Synnott, S. P., & Null, G. W. 1998, in Modern Astrometry and Astrodynamics, ed. R. Dvorak, H. F. Haupt, & K. Wodnar (Vienna: Verlag Österreichischer Akad. Wiss.), 89
Rapaport, M., et al. 2001, A&A, 376, 325
Russell, J. L., Lasker, B. M., McLean, B. J., Sturch, C. R., & Jenkner, H. 1990, AJ, 99, 2059
Standish, E. M. 1998, JPL Planetary and Lunar Ephemerides, DE405/LE405 (Interoffice Memo. 312.F-98-048) (Pasadena: JPL)
Stobie, R. S. 1980, Proc. SPIE, 264, 208
Stone, R. C. 1984, A&A, 138, 275
———. 1994, AJ, 108, 313
———. 1996a, PASP, 108, 1051
———. 1996b, AJ, 112, 781
———. 1997a, AJ, 113, 2317
———. 1997b, in IAU Colloq. 165, Dynamics and Astrometry of Natural and Artificial Celestial Bodies, ed. I. M. Wytrzyszczak, J. H. Lieske, & R. A. Feldman (Dordrecht: Kluwer), 535
———. 1997c, AJ, 114, 850
———. 1997d, AJ, 114, 1679
———. 1997e, AJ, 114, 2811
———. 1998a, AJ, 116, 1461
———. 1998b, ApJ, 506, L93
———. 2000a, AJ, 120, 2124
———. 2000b, AJ, 120, 2708
———. 2001, AJ, 122, 2723
———. 2002, PASP, 114, 1070
Stone, R. C., & Harris, F. H. 2000, AJ, 119, 1985
Stone, R. C., McDonald, S. W., & Elliot, J. L. 1999a, AJ, 118, 591
Stone, R. C., McDonald, S. W., Elliot, J. L., & Bowell, E. 2000, AJ, 119, 2008
Stone, R. C., Monet, D. G., Monet, A. K. B., Walker, R. L., Ables, H. D., Bird, A. R., & Harris, F. H. 1996, AJ, 111, 1721
Stone, R. C., Pier, J. R., & Monet, D. G. 1999b, AJ, 118, 2488
Urban, S. E., Corbin, T. E., & Wycoff, G. L. 1998, AJ, 115, 2161
Zacharias, N., et al. 2000, AJ, 120, 2131